EARTH SURFACE PROCESSES AND LANDFORMS
*Earth Surf. Process. Landforms* **35**, 136–156 (2010)

Published online 10 December 2009 in Wiley InterScience
(www.interscience.wiley.com) DOI: 10.1002/esp.1886

# Accounting for uncertainty in DEMs from repeat topographic surveys: improved sediment budgets

**Joseph M. Wheaton[1], James Brasington[2], Stephen E. Darby[3] and David A. Sear[3]**
[1] Department of Watershed Sciences, Utah State University, 5210 Old Main Hill, NR 210, Logan, UT 84322, USA
[2] Institute of Geography & Earth Sciences, Aberystwyth University, Aberystwyth, SY23 3DB, UK
[3] School of Geography, University of Southampton, Highfield, Southampton, SO17 1BJ, UK

Received 22 September 2008; Revised 26 June 2009; Accepted 6 July 2009

Correspondence to: Joseph M. Wheaton, Department of Watershed Sciences, Utah State University, 5210 Old Main Hill, NR 210, Logan, UT 84322, USA.
E-mail: Joe.Wheaton@usu.edu

ESPL
Earth Surface Processes and Landforms

ABSTRACT: Repeat topographic surveys are increasingly becoming more affordable, and possible at higher spatial resolutions and over greater spatial extents. Digital elevation models (DEMs) built from such surveys can be used to produce DEM of Difference (DoD) maps and estimate the net change in storage terms for morphological sediment budgets. While these products are extremely useful for monitoring and geomorphic interpretation, data and model uncertainties render them prone to misinterpretation. Two new methods are presented, which allow for more robust and spatially variable estimation of DEM uncertainties and propagate these forward to evaluate the consequences for estimates of geomorphic change. The first relies on a fuzzy inference system to estimate the spatial variability of elevation uncertainty in individual DEMs while the second approach modifies this estimate on the basis of the spatial coherence of erosion and deposition units. Both techniques allow for probabilistic representation of uncertainty on a cell-by-cell basis and thresholding of the sediment budget at a user-specified confidence interval. The application of these new techniques is illustrated with 5 years of high resolution survey data from a 1 km long braided reach of the River Feshie in the Highlands of Scotland. The reach was found to be consistently degradational, with between 570 and 1970 $m^3$ of net erosion per annum, despite the fact that spatially, deposition covered more surface area than erosion. In the two wetter periods with extensive braid-plain inundation, the uncertainty analysis thresholded at a 95% confidence interval resulted in a larger percentage (57% for 2004–2005 and 59% for 2006–2007) of volumetric change being excluded from the budget than the drier years (24% for 2003–2004 and 31% for 2005–2006). For these data, the new uncertainty analysis is generally more conservative volumetrically than a standard spatially-uniform minimum level of detection analysis, but also produces more plausible and physically meaningful results. The tools are packaged in a wizard-driven Matlab software application available for download with this paper, and can be calibrated and extended for application to any topographic point cloud (x,y,z). Copyright © 2009 John Wiley & Sons, Ltd.

KEYWORDS: DEM of Difference (DoD); fluvial geomorphology; morphological method; morphological sediment budgeting; River Feshie; fuzzy inference system

## Introduction

With recent advances in ground-based, boat-based and remotely-sensed surveying technologies, the rapid acquisition of topographic data is now possible at spatial resolutions and extents previously unimaginable (Lane and Chandler, 2003; Heritage and Hetherington, 2007; Milan *et al.*, 2007; Marcus and Fonstad, 2008; Notebaert *et al.*, 2008). These advances make monitoring geomorphic changes and estimating sediment budgets through repeat topographic surveys and the application of the morphological method (Church and Ashmore, 1998) a tractable, affordable approach for monitoring applications in both research and practice. In fluvial geomorphology, the morphological approach has been used as an alternative to measuring sediment transport directly and has historically been applied primarily to repeat surveys of river plan form, cross-sections and/or longitudinal profiles (Brewer and Passmore, 2002; Lane, 1998). However, from the early 1990s (Lane *et al.*, 1994), the morphological method has been expanded to include the use of repeat topographic surveys from which digital elevation models (DEMs) could be constructed and differenced to produce DEMs of Difference (DoDs). This paper focuses exclusively on the 2D application of the morphological method using DoDs.

Uncertainty in DoD application of the morphological method has already received considerable attention (Lane *et al.*, 1994; Milne and Sear, 1997; Brasington *et al.*, 2000; Lane, 1998; Lane *et al.*, 2003). Driving this interest has been the basic question that, given the uncertainty inherent in individual DEMs, is it possible to distinguish real geomorphic changes from noise? Repeat surveys using rtkGPS (Brasington *et al.*, 2000), total stations (Milne and Sear, 1997), aerial photogrammetry (Winterbottom and Gilvear, 1997; Westaway *et al.*, 2001), multi-beam echo-sounding (Calder and Mayer,

2003), airborne LiDaR (Cavalli *et al.*, 2008), and airborne narrow-beam terrestrial-aquatic green LiDaR (McKean *et al.*, 2008) have notional accuracies in surface elevations of anywhere from ±0·02 m to ±1 m (Fuller *et al.*, 2003; Glenn *et al.*, 2006; Carter *et al.*, 2007). For the fluvial environment, which commonly exhibits topographic changes of a similar magnitude to this noise, how well these uncertainties are accounted for determines what (if anything) can meaningfully be interpreted from such surveys (Brasington *et al.*, 2003; Lane *et al.*, 2003). Particularly when surveying submerged topography in rivers, elevation uncertainties can be even higher (Sear and Milne, 2000; Lane *et al.*, 2003). With recent improvements in surveying technologies, acquisition times have been cut by orders of magnitude (Marcus and Fonstad, 2008). This allows the collection of more data, at higher time-and-space resolution and over greater spatial extents. For this additional data to be useful, an effective, robust technique for quantifying uncertainty is required.

Estimates of the net change in storage terms for morphologically inferred sediment budgets are fundamentally controlled by DEM quality, which itself is largely inherited by the quality of the survey data. DEM quality is an unknown function of survey point quality, sampling strategy, surface composition, topographic complexity and interpolation methods (Wise, 1998; Wechsler, 2003; Wechsler and Kroll, 2006). Despite community awareness of such issues, most estimates of the influence of DEM uncertainty on DoDs are relatively simplistic in that they assume uncertainties are either spatially uniform (Brasington *et al.*, 2000) or that they vary spatially only on the basis of wet and dry areas (Lane *et al.*, 2003). Consequently, quantified uncertainties are sometimes unnecessarily conservative in areas where very small magnitude changes might be occurring (e.g. relatively smooth floodplain surfaces) and overly liberal in areas experiencing high magnitude elevation changes (e.g. eroding banks).

The most commonly adopted procedure for managing DEM uncertainties involves specifying a minimum level of detection threshold ($_{min}$LoD) to distinguish actual surface changes from the inherent noise (Fuller *et al.*, 2003). Predicted elevation changes that occur beneath this detection limit are typically discarded, or their probability of being real adjusted using a simple declining weighting function (Lane *et al.*, 2003, p. 252). Typically, elevation changes above this $_{min}$LoD are treated as real. There is, however, some inconsistency as to whether the propagated error used to estimate the $_{min}$LoD should also be applied to changes over a threshold (e.g. if a $_{min}$LoD of 10 cm was defined and the change was 15 cm, should it be 15 cm or 15 cm +/– 10 cm?). Determination of the $_{min}$LoD requires both a theory of change detection and a metric of DEM quality (Brasington *et al.*, 2000; Lane *et al.*, 2003). Typically, this is addressed applying the classical statistical theory of errors (Taylor, 1997) taking a measure of DEM precision derived from check data as a surrogate for DEM quality (Milan *et al.*, 2007).

The purpose of this paper is to present a new technique that allows more robust estimation of DEM quality and its influence on sediment budgets derived from DEM differencing. Therein, the spatial variability of surface representation uncertainty is considered using a set of tools that could be calibrated and applied to any set of topographic point data. Our approach builds on the conceptual frameworks for uncertainty analysis in the morphological method established by Brasington *et al.* (2000) and Lane *et al.* (2003). The novel contributions set out here are: (i) a new technique for estimating the magnitude of DEM uncertainty in a spatially variable way using fuzzy set theory; and (ii) a technique for discriminating DoD uncertainty on the basis of the spatial coherence of erosion and deposition units using Bayes Theorem. These tools are packaged together into a Matlab software application available for download as supporting information for this article.

The paper is organized as follows. First the River Feshie study site used in this paper is introduced with an explanation of the DoD data to be used. Then a brief review of the theoretical framework behind DEM differencing and uncertainty accounting is presented. Next the theory for the extension of these techniques and substantive methodological contribution is introduced. Finally, the application of the new method is illustrated. The paper closes with a discussion of the main findings, limitations and what improvements can be made in the future.

## River Feshie study site

To develop this new technique, a data set of high-resolution repeat topographic surveys from a system that was sufficiently dynamic to exhibit a range of styles of geomorphic change over a reasonable duration study period (e.g. 3 or more years) was desirable. Thomas (2006, Chapter 7) identified seven rivers where data were emerging from such intensive high resolution monitoring campaigns, but only five with repeat survey data, including the Feshie. Although other data sets exist, few, if any, ground-based survey data sets in the world match the detail and temporal scope of that started by Brasington *et al.* (2000) from the River Feshie in the Cairngorm Mountains of Scotland (Wheaton, 2008).

The River Feshie drains a 231 km$^2$ catchment with 1030 m of relief in the heart of the Scottish Highlands. The specific study site stretches over ~1 km of an unconfined 3-km-long braided reach within Glenfeshie (Figure 1), where the active braidplain varies between 50 and 250 m in width. The Glen itself is a glacial trough, which was deglaciated roughly 13 000 BP (Gilvear *et al.*, 2000) leaving behind a large fluvio-glacial fill that is regularly reworked by the unregulated and flashy flow-regime of the Feshie (Ferguson and Werritty, 1983; Soulsby *et al.*, 2006). In a British context, the Feshie is exceptionally dynamic and has accordingly been the subject of numerous geomorphological (Werrity and Ferguson, 1980; Ferguson and Werritty, 1983; Robertson-Rintoul, 1986; Brazier and Ballantyne, 1989; Ferguson and Ashworth, 1992; Brasington *et al.*, 2000; Gilvear *et al.*, 2000; Rumsby *et al.*, 2001; Brasington *et al.*, 2003; Rumsby *et al.*, 2008), hydrological (Soulsby *et al.*, 2001; Rodgers *et al.*, 2004; Rodgers *et al.*, 2005; Soulsby *et al.*, 2006), and geological (Young, 1976; Bremner, 1915) studies.

## Feshie DoDs: 2003 to 2007

For the purposes of this paper, annual summer topographic survey data were analysed from 2003 to 2007. The 2003 through 2006 surveys were derived entirely from rtkGPS surveys whereas the 2007 data set was augmented with total station data. Each survey comprised between 34 000 and 51 000 points over an 11·5 to 14·5 ha survey area (Table I). A total of 248 266 ground-based survey points were acquired of which 2622 points in 2007 were collected using a Leica TCRP 1205 robotic total station. The remaining data points were collected with Leica System 1200 and Trimble R8 differential GPS rovers running in realtime kinematic (RTK) mode communicating to a base station occupying a known control point on a local grid coordinate system that approximates the Ordnance Survey's British National Grid. The average kernel point density (pt ρ) was on the order of 0·3 points m$^{-2}$ (based

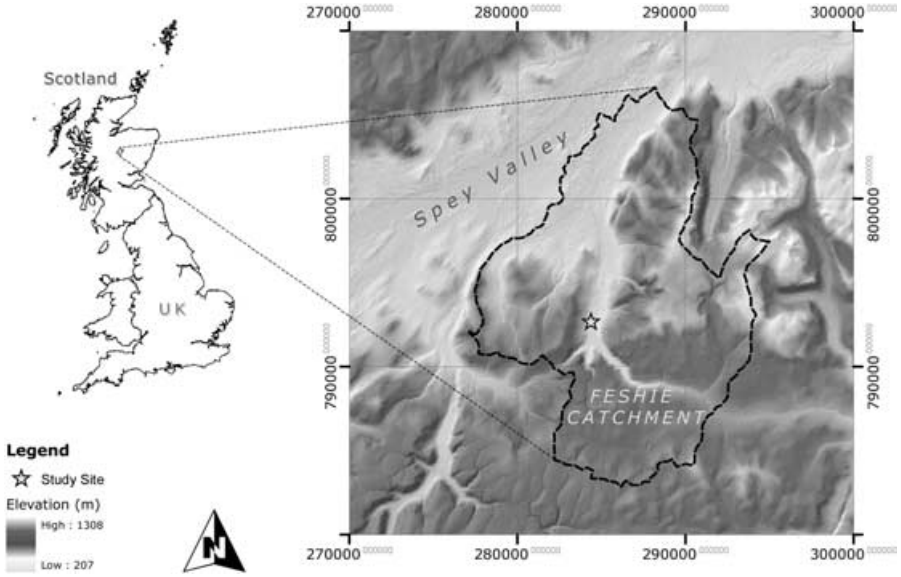


**Figure 1.** Location map for River Feshie study site.

**Table I.** Survey point density statistics. The total number of points surveyed are reported in the second column, whereas those used for analyses (intersection of all survey areas) are reported in the third column. Statistics for point density (pt ρ) are based on a global calculation (columns 4 and 5) and a 5 × 5 moving window average are reported in the columns 6 through 8

| | Points surveyed (*n*) | | Global pt ρ (pts $m^{-2}$) | | Moving window pt ρ (pts $m^{-2}$) | | |
|---|---|---|---|---|---|---|---|
| Survey | Total | Analysis clip | Total | Analysis clip | Mean | Max | σ |
| 2003 | 51080 | 33811 | 0·51 | 0·29 | 0·40 | 4·56 | 0·32 |
| 2004 | 48145 | 32675 | 0·38 | 0·28 | 0·37 | 2·52 | 0·28 |
| 2005 | 35536 | 23258 | 0·26 | 0·20 | 0·26 | 2·92 | 0·21 |
| 2006 | 37861 | 23258 | 0·26 | 0·20 | 0·29 | 4·11 | 0·17 |
| 2007 | 34266 | 27592 | 0·24 | 0·24 | 0·24 | 2·64 | 0·17 |
| Average | 41378 | 28119 | 0·33 | 0·24 | 0·31 | 3·35 | 0·23 |

**Table II.** Gross DoD budget results (no uncertainty accounting)

| | Volumetric | | | Percentage coverage of reach | | |
|---|---|---|---|---|---|---|
| DoD period | Erosion $m^3$ | deposition $m^3$ | Net change $m^3$ | Erosion % | Deposition % | Total % |
| 2007–2006 | 11162·0 | 8882·3 | –2279·7 | 50·2% | 49·5% | 99·7% |
| 2006–2005 | 4538·5 | 3167·1 | –1371·3 | 54·1% | 45·0% | 99·0% |
| 2005–2004 | 8307·9 | 7029·7 | –1278·2 | 46·8% | 52·5% | 99·2% |
| 2004–2003 | 4975·5 | 3072·2 | –1903·3 | 56·4% | 43·2% | 99·5% |

on a 5 × 5 rectangular moving window; see Table I). A 2–3 m grid-based sampling scheme was adopted across the entire reach, with feature-stratified infilling in areas of greater topographic complexity to capture bar-scale morphological features (Valle and Pasternack, 2005). In general, this results in high point density in areas of topographic complexity and low point density in topographically simple areas.

DEMs were constructed in ESRI's ArcGIS using a simple workflow in which survey points were used to derive a triangular irregular network (TIN) using Delaunay triangulation, which was then linearly resampled onto a grid of user-specified resolution. Survey points were first filtered to remove any visually obvious anomalies and then further filtered to remove points with an instrument-calculated GPS, 3D point qualities below +/– 5 cm (mean 3D point quality was 1·7 cm). A hard clip polygon was drawn around the surveyed points and used in TIN construction to prevent spurious interpolation beyond the survey area. A 1 m resolution DEM was used throughout the analyses reported herein, which was deemed to be an appropriate compromise between computational efficiency, information loss, and sufficient resolution to resolve bar-scale morphology. The resulting five DEMs are shown at the top of Figure 2. Four DoDs were calculated from these DEMs by simply subtracting the elevations in each DEM on a cell-by-cell basis, from those in the DEM from the next year's survey (bottom of Figure 2). Estimates of net volumetric change were then approximated using a simple integration scheme, multiplying the calculated elevation change (a depth measurement) by the surface area of each cell (i.e. 1 $m^2$). These volumes were then summed into erosional and depositional categories to produce a net volumetric budget.

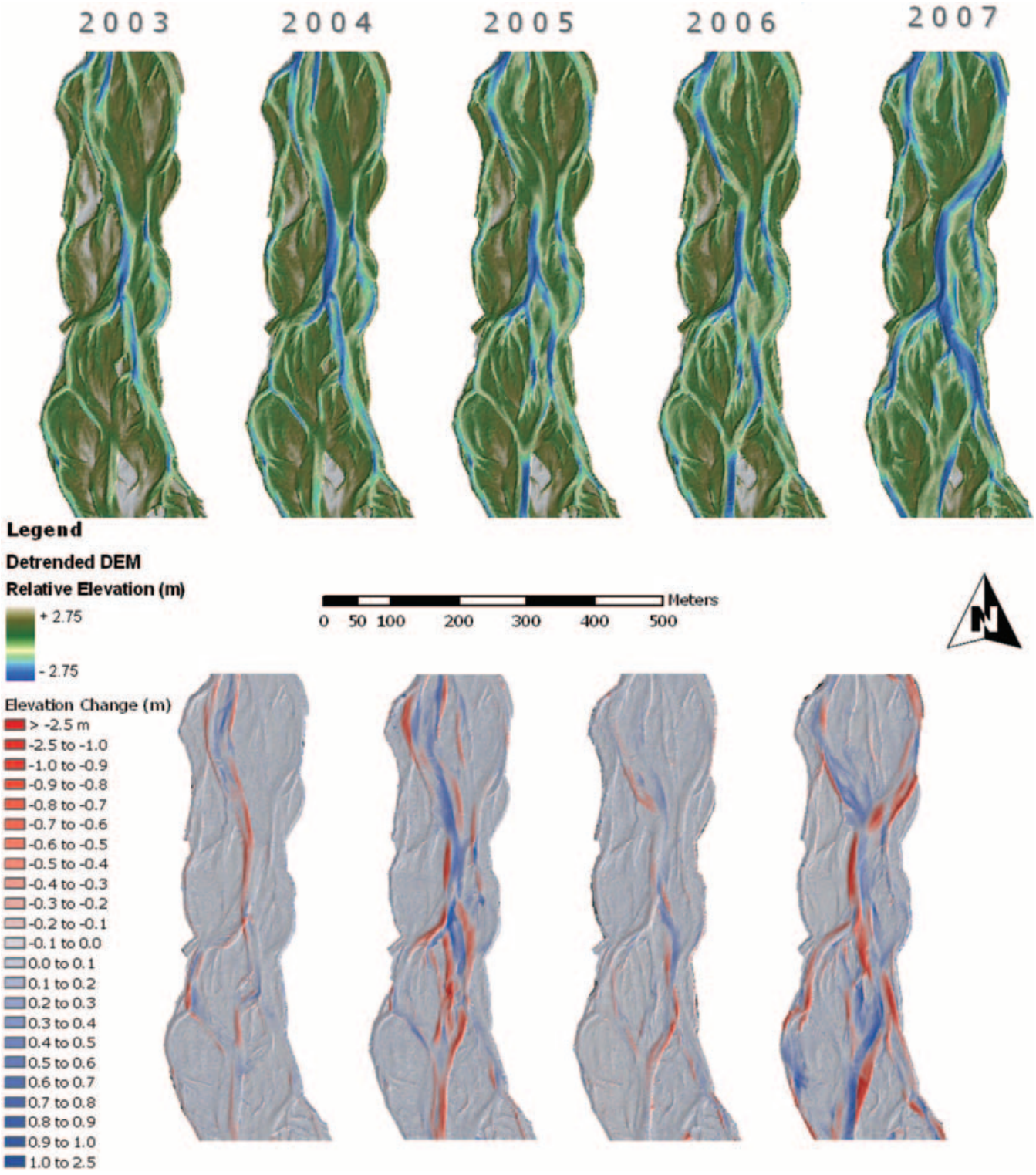


**Figure 2.** Detrended DEMs and DoD for 2003 to 2007. Note that the hillshades from the more recent year in the DoD are shown behind the DoD for context. This figure is available in colour online at www.interscience.wiley.com/journal/espl

Table II highlights the gross volumetric budgets derived from this analysis. Columns 5–7 of Table II show the percentages of surface area of the reach experiencing erosion and deposition with no accounting of measurement precision or detection thresholds (other than that implied by the number of significant figures shown). This analysis suggests that over 99% of the reach experiences changes in all four periods. However, over the 5-year study period, the entire survey reach was never completely inundated and there are substantial zones of elevated, vegetating and/or vegetated bar surfaces, terraces and islands (see Appendix B of Wheaton, 2008). In areas where no agent for geomorphic change was experienced (i.e. high island and terrace surfaces not subject to inundation, flooding or significant overland flow), evidence for change is clearly questionable. However, small elevation differences are not surprising and reflect a combination of random surveying errors (e.g. GPS triangulation errors, pole tilt, etc.), systematic errors (e.g. resection errors, interpolation errors, incorrect survey rod height, etc.), the limits of the instrument precision, operator blunders, and sampling differences between surveys. The challenge in areas where geomorphic changes have taken place, is to untangle those differences from this background

noise. It is interesting to note that the total volumetric change throughout the study period (Column 4 of Table II) suggests that the reach is consistently degradational with net erosion of between 1200 and 2300 $m^3$ each year, comprising 8% and 24% of the total volume of estimated change. By contrast, the areal percentage summaries for 2004 to 2005 suggest that in terms of surface area, more of the reach was aggradational than depositional.

## Existing Approaches to Characterizing DEM Uncertainty

There are a number of existing approaches to quantifying the influence of surface representation uncertainty on sediment budgets derived from DEM differencing. Regardless of the approach used, the process of accounting for DoD uncertainty follows a consistent progression through three steps:

1. quantifying the surface representation uncertainty in the individual DEM surfaces that are being compared;
2. propagating the identified uncertainties into the DoD;
3. assessing the significance of the propagated uncertainty.

In the next three subsections, these steps are briefly reviewed to highlight where methodological gaps exist (for a more detailed review, see Wheaton, 2008, Chapter 4).

### Quantifying surface representation uncertainty

There are a variety of ways to quantify uncertainties in the vector topographic survey data (i.e. x,y,z point clouds) manifest in DEMs. Here, this uncertainty will be denoted as $\delta z$. We know that the horizontal components of this positional error are of a similar magnitude to the vertical components, but they have negligible influence on vertical surface differences in low slope areas (i.e. most fluvial environments). Treating the horizontal components as negligible, $\delta z$ is related to the actual elevation $Z_{Actual}$ as follows:

$$Z_{Actual} = Z_{DEM} \pm \delta z \quad (1)$$

where $Z_{Actual}$ is the true value of elevation, and $Z_{DEM}$, the spatially-paired DEM elevation.

Approaches for approximating $\delta z$ range from adopting a manufacturer reported instrument precision to attempts at composing complete error budgets (Lichti *et al.*, 2005). In fact, manufacturer reported precision is only one of many components of $\delta z$, which include measurement errors, sampling bias (density and sampling patterns) and interpolation methods. By contrast, complete error budgets require data collection and testing protocols that go beyond typical survey practice. Other techniques for estimating $\delta z$ include repeat observation of control points (Brasington *et al.*, 2000) (Table III), bootstrapping experiments (Wheaton, 2008), repeat surveys of unchanging surfaces (Wheaton, 2008), fuzzy terrain models (Lodwick and Santos, 2003) and more traditional geostatistical techniques like surface interpolation with Kriging surfaces (Chappell *et al.*, 2003).

Although pin-pointing the precise magnitude of $\delta z$ requires information beyond the topographic data itself, it is known that $\delta z$ tends to exhibit patterns in its spatial variability that are coherent and predictable (Wheaton *et al.*, 2004). Later in this paper we exploit this observation to develop a technique for estimating $\delta z$ that requires only the raw topographic data.

**Table III.** Variance in repeat GPS observation of control points over 3 years ($n$ = 382 observations). Standard deviations ($\sigma$) of each coordinate component were calculated for each control point and then averaged over the number of control points to produce $\sigma_\mu$. The fifth column shows an average standard deviation for each coordinate component that was weighted by the number of observations from that year (row 5). The higher variance reported in 2005 was likely due to repeat control observations

| | 2004 | 2005 | 2006 | Combined |
|---|---|---|---|---|
| $\sigma_\mu$ Easting (m) | 0·015 | 0·034 | 0·007 | 0·020 |
| $\sigma_\mu$ Northing (m) | 0·014 | 0·037 | 0·012 | 0·020 |
| $\sigma_\mu$ Elevation (m) | 0·007 | 0·018 | 0·004 | 0·010 |
| No of Repeat observations | 257 | 110 | 15 | 382 |
| No of Control points | 6 | 5 | 5 | 16 |

### Propagating uncertainty into DoD

Brasington *et al.* (2003) showed the individual errors in the DEMs can be propagated into the DoD as:

$$\delta u_{DoD} = \sqrt{(\delta z_{new})^2 + (\delta z_{old})^2} \quad (2)$$

where $\delta u_{DoD}$ is the propagated error in the DoD, and $\delta z_{new}$ and $\delta z_{old}$ are the individual errors in $DEM_{new}$ and $DEM_{old}$, respectively. This method assumes that errors in each cell are random and independent. The combined error can be calculated as a single value for the entire DoD if spatially-explicit estimates of $\delta z_{new}$ and $\delta z_{old}$ do not exist. Alternatively, spatial variability in $\delta z$ can be considered for both DEMs independently and $\delta u_{DoD}$ can be calculated on a region by region (Lane *et al.*, 2003; Westaway *et al.*, 2003) or cell-by-cell basis (Wheaton, 2008). While simple region filters such as submerged (wet) versus un-submerged (dry) areas, are straightforward to apply, objective techniques for a more detailed and cell-by-cell estimate of $\delta z$ have been lacking.

### Assessing the significance of DoD uncertainty

There are two primary ways in which the significance of uncertainties in DoD predicted elevation changes are typically expressed. Both rely on thresholding the DoD and discarding or applying a lower weighting to elevation changes below some detection limit (i.e. $_{min}$LoD). In the first simple approach, the propagated uncertainties (i.e. $\delta u_{DoD}$) are used to define a threshold elevation change, or $_{min}$LoD (with dimensions of length; e.g. +/– 10 cm). For example, a $_{min}$LoD of 10 cm could correspond to two DEMs with equal $\delta z$ of 7·07 cm using Equation (2). Both the volumetric and areal estimates of morphological change are highly sensitive to the $_{min}$LoD, as illustrated with DoD data from 2006 to 2007 on the River Feshie (Figure 3). The more uncertain the DEMs (and hence the higher the $_{min}$LoD threshold), the more information is lost from the budget. Thus, the significance of the uncertainty manifested in $\delta u_{DoD}$ is the inability to reliably detect elevation changes below the $_{min}$LoD threshold.

As an alternative, Brasington *et al.* (2003) and Lane *et al.* (2003) draw on Taylor (1997) to show how probabilistic thresholding can be carried out with a user-defined confidence interval. If the estimate of $\delta z$ is a reasonable approximation of the standard deviation of error (*SDE*), Equation (2) can be modified to:

$$U_{crit} = t\left(\sqrt{SDE_{new}^2 + SDE_{old}^2}\right) \quad (3)$$

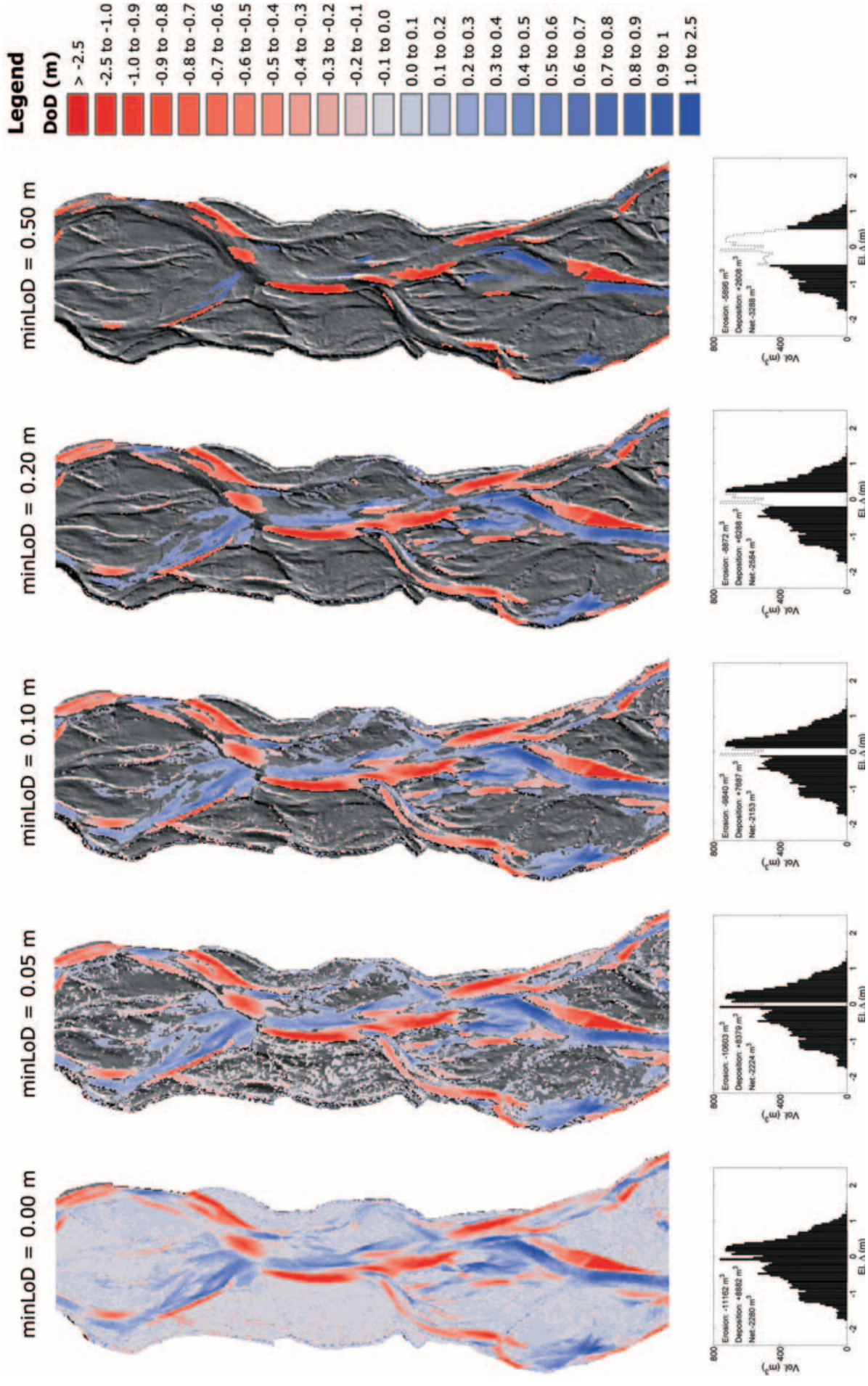


**Figure 3.** Example of significance of elevation $_{min}$LoD threshold on DoD budget for 2007–2006 DoD. The DoD maps are shown on top and the elevation change distributions (ECDs) are shown below. The gross unthresholded DoD is shown on the far left, and moving toward the right progressively more conservative (i.e. higher $\delta z$ and $_{min}$LoD) are shown. This figure is available in colour online at www.interscience.wiley.com/journal/espl

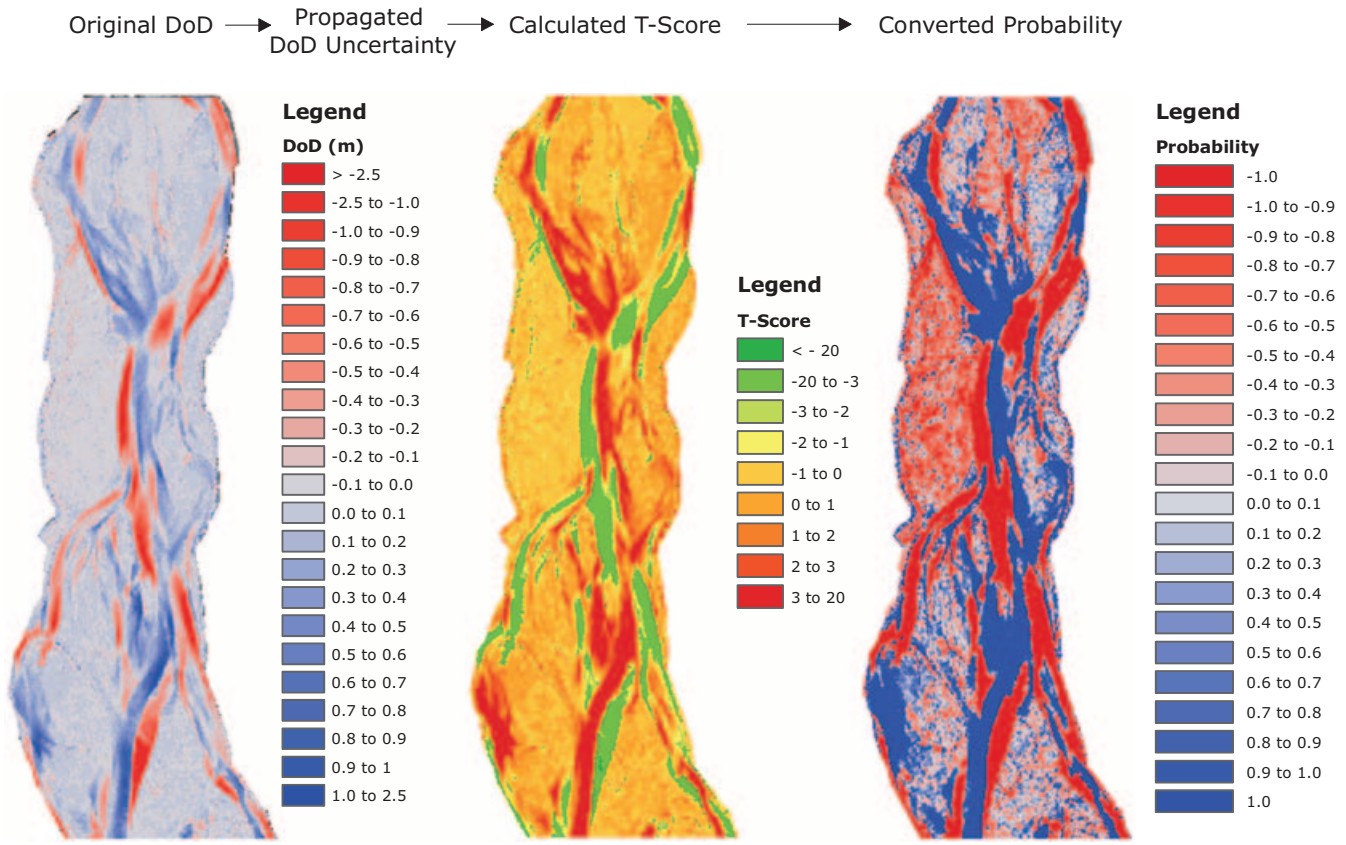


**Figure 4.** Illustration of the calculation of the probability that DoD predicted changes are real for 2006–2005 DoD. Given a DoD (left), and some spatially uniform propagated DoD uncertainty (calculated as 0·085 cm in this example from Equation (2): $0{\cdot}085 = \sqrt{0{\cdot}06^2 + 0{\cdot}06^2}$), a T-score can be calculated directly from Equation (4) (middle), and then converted to a probability (right). Both positive and negative probabilities are shown, with erosional probabilities denoted by a negative sign to distinguish them from depositional probabilities (positive). This figure is available in colour online at www.interscience.wiley.com/journal/espl

where $U_{crit}$ is the critical threshold error, based on a critical student's *t*-value at a chosen confidence interval where

$$t = \frac{|z_{DEM_{new}} - z_{DEM_{old}}|}{\delta u_{DoD}} \quad (4)$$

In Equation (4), $|z_{DEM_{new}} - z_{DEM_{old}}|$ is simply the absolute value of the DoD. The probability of a DoD predicted elevation change occurring purely due to chance measurement error can then be calculated by relating the *t*-statistic to its cumulative distribution function (CDF). Throughout this paper, the 95% confidence interval is used as a threshold. An example of probabilities derived using this technique from spatially uniform estimates of $\delta z$ is shown in Figure 4. Following this method, an error-reduced DoD can then be obtained by discarding all changes with probability values less than the chosen threshold. In practice it is just as easy to apply a confidence-interval based threshold from spatially uniform versus spatially variable estimates of $\delta z$. However, objectively estimating a spatially variable $\delta z$ is the major challenge.

## Methodological Development

If spatially uniform $_{min}$LoD analyses result in true geomorphic changes being discarded, knowledge of the spatial structure of elevation uncertainty becomes fundamentally important. Specifically, if regions of the DoD where $\delta z$ is lower than currently presumed can be identified, a less restrictive $_{min}$LoD may be applied locally and more information recovered (particularly relevant where deposition on bar tops occurs as broad shallow gravel sheets). Similarly, in areas where $\delta z$ is substantially higher than currently presumed (e.g. steep banks), a more restrictive $_{min}$LoD may be applied to more accurately adjust volumetric estimates of change to reflect this higher uncertainty. As Brasington *et al.* (2003) pointed out, the problem with a spatially uniform $_{min}$LoD is that it influences different processes in different ways. A process like bank erosion has an elevation change distribution (ECD) that is entirely erosional but spans a large range of elevation change magnitudes (reflecting primarily differences in bank heights). In contrast, a process like overbank deposition tends to exhibit a peaked ECD concentrated toward low-magnitude elevation changes that may well fall below a $_{min}$LoD threshold. To address these issues, two methodological innovations are presented in the sections below – quantifying spatially variable uncertainties and accounting for spatial coherence of change.

### Spatially variable uncertainty quantification

Repeat surveys of unchanging surfaces performed on the Feshie by Wheaton (2008) revealed a strong and predictable spatial bias in elevation uncertainty. Essentially, areas that are steep, have low survey point density and high surface roughness (e.g. cobbles and boulders), have very high elevation uncertainty; whereas areas that are flat, have relatively high survey point density and are smooth have low elevation uncertainty. When elevation uncertainty is treated as spatially uniform, the $_{min}$LoD is typically either defined based on an average value, which tends to discard more information than it should in areas where elevation uncertainty is low, and not enough information in areas where elevation uncertainty is high. When a more conservative approach is employed (i.e.

a higher $_{min}$LoD), even more information about true geomorphological changes are discarded. These simple observations form the premise for developing methods that aim to quantify the spatial variability of elevation uncertainty. The crux of the problem is that the various components of elevation uncertainty are collinear variables and do not exhibit a simple monotonic relationship to elevation uncertainty. Although an expert can identify the various factors that contribute to uncertainty, a deterministic model cannot be unambiguously constructed. For these reasons, a more heuristic approach was attempted here.

Whereas probabilistic models primarily describe *random variability* in parameters, fuzzy models primarily deal with *vagueness* in parameters (Chen *et al.*, 1999). Although the assumptions on the nature of the statistics (e.g. independence of variables, errors being random) underlying probabilistic models of uncertainty can be stretched in order to apply them, such applications may lead to serious errors (Chen *et al.*, 1999). By contrast, fuzzy models require very few assumptions and can be applied when relatively little is known about the uncertainty, or what is known can only be articulated in less precise linguistic terms (Bandemer and Gottwald, 1995; Klir and Yuan, 1995). One of the subsets of fuzzy set theory is fuzzy logic, and one of the tools that grows out of fuzzy logic is the fuzzy inference system (Klir and Yuan, 1995).

Fuzzy logic is often described as a trade-off between significance and precision (Jang and Gulley, 2007). This is important as the geomorphologist may not necessarily need to know the precise magnitude of elevation uncertainty in each component of the error budget (e.g. errors due to slightly tilted survey pole) rather, the significance of the total uncertainty on the geomorphic interpretation. Fuzzy inference systems are convenient frameworks for taking the information that is known (inputs) and producing an appropriate output (Jang and Gulley, 2007). In the case of topographic surveys, something is always known about the survey sampling (e.g. point density) and the morphology (slope), and in some cases there may be additional information (e.g. roughness from facies maps, point quality from GPS). From empirical research (Wheaton, 2008), we have an approximate understanding of the range and general magnitude of elevation uncertainties associated with various types of land surveying. Here, a fuzzy inference system (FIS) was developed that accepts the inputs that are readily available and produces a $\delta z$ output that is calibrated to the range of empirically determined values. Matlab's Fuzzy Logic Toolbox, developed by Jang and Gulley (2009), was used to implement this FIS.

The fuzzy inference system consists of four components:

1. specification of FIS type, fuzzy operation methods, rule implication method (and vs. or), aggregation method (min vs. max) and defuzzification method (if applicable);
2. definition of fuzzy membership functions for the inputs;
3. definition of rules relating inputs to outputs;
4. definition of fuzzy membership function for the output;

The most common default specifications suggested by Jang and Gulley (2007) were used for FIS type *Mamandi*. The fuzzy operation methods refer to how inputs for rules are combined (using Boolean operators), whereas the rule implication method refers to how a output membership function is arrived at for each rule (minimum method used). The aggregation method refers to how the outputs from all applicable rules are combined into a single output membership function (maximum method used). Finally the defuzzification method refers to how the fuzzy number output (a membership function), can be converted into a crisp, single-value number (centroid method used). The next sub-section addresses the second and third components and the following subsection addresses the fourth component.

### Fuzzy inputs and output

Although fuzzy membership functions come in a wide array of forms, the most common are triangular and trapezoidal membership functions. Although FIS outputs tend not to show significant sensitivity to membership function shape (Klir and Yuan, 1995). The process of defining membership functions can be thought of in two parts. First, the number of linguistic adjectives that could be used to describe each variable needs to be identified. For the inputs used here (slope, point density and point quality), the simple adjectives 'high', 'medium' and 'low' were deemed adequate. The second part consists of defining the membership function that describes the range of values covered by each adjective. The membership functions used here are shown in Figure 5. For the input variables, so long as the membership functions span the range of encountered values for that variable, the exact specification of their membership function is not critical (Jang and Gulley, 2007; Klir and Yuan, 1995). What is more important is that the expert defining the rule system knows what values the adjectives correspond to and develops rules in accordance with those perceptions. For the output variable ($\delta z$ in this case), the output membership functions must correspond to realistic output values. Outputs from the FIS were calibrated to values found in empirical experiments on the Feshie reported in Wheaton (2008). These experiments surveyed a subsection of the reach five times within a day during a period when no geomorphic changes took place. The subsection spanned the full range of morphological unit types, roughness types, slopes and survey sampling styles exhibited in the larger study area. As such, variance between DEMs from these five surveys provided an excellent spatially stratified data set to calibrate the FIS system.

### FIS rules

Rule definition for the FIS is a process of linguistically relating the inputs (using their different adjectives defined above) to a single adjective for the output. For example, if 3D point quality is high, slope is low, and point density is high, then elevation uncertainty is low. By contrast if 3D point quality is low, slope is high, and point density is low, then elevation uncertainty is extreme. The complete 3-input rule system used in this paper is shown in Table IV. A more generic 2-input rule FIS system applicable to any topographic survey based on just slope and point density is reported in Wheaton (2008, Table 4.7).

### Application of FIS

A fuzzy inference diagram is the standard technique for illustrating how a specific fuzzy inference system operates. In Figure 6 an illustration of the 2-rule FIS is shown. Two examples are shown here to contrast the outputs from different point density and slope inputs. The first step in applying the FIS involves the calculation of the output membership function for each applicable individual rule (implication method). Not all rules will apply. In the example of Figure 6A only one rule from five candidate rules of the nine total rules applies (i.e. if slope is low and point density high then elevation uncertainty is low). Whereas in Figure 6B, two of six candidate rules of the nine total rules are applicable. Next, the total consequence of all the applicable rules is calculated (termed the aggregation method). This resulting total consequence membership function expresses the full range of uncertainty in the output predicted by the FIS. Finally, if desired, the total consequence membership function can be defuzzified into a crisp output

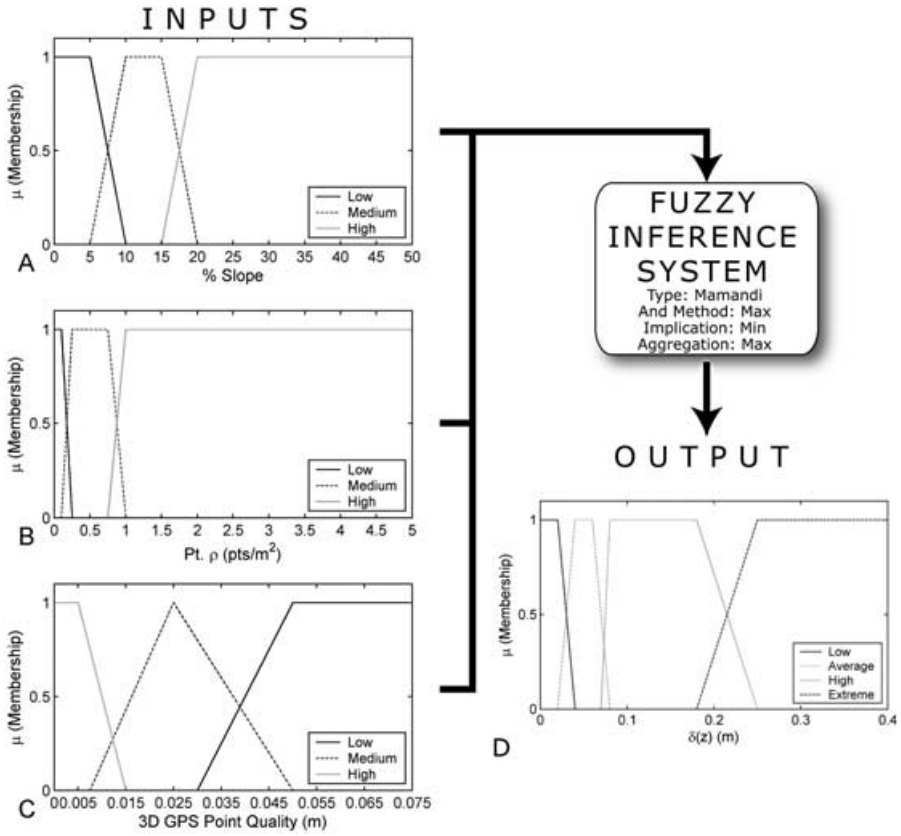


**Figure 5.** Input and output fuzzy membership functions used in this paper. Inputs: (A) slope; (B) point density; and (C) point quality. Output: (D) elevation uncertainty $\delta z$.

**Table IV.** Three input fuzzy inference system for elevation uncertainty ($\delta$(z)). The three inputs are GPS-reported 3D point quality, percentage slope and point density

| | Inputs | | | Output |
|---|---|---|---|---|
| Rule | 3D P.Q. m | Slope % | Pt. ρ Pts $m^{-2}$ | $\delta$(z) m |
| 1 | High | Low | High | Low |
| 2 | High | Medium | High | Average |
| 3 | High | High | High | High |
| 4 | High | Low | Medium | Low |
| 5 | High | Medium | Medium | Average |
| 6 | High | High | Medium | High |
| 7 | High | Low | Low | Average |
| 8 | High | Medium | Low | High |
| 9 | High | High | Low | Extreme |
| 10 | Medium | Low | High | Low |
| 11 | Medium | Medium | High | Average |
| 12 | Medium | High | High | High |
| 13 | Medium | Low | Medium | Average |
| 14 | Medium | Medium | Medium | High |
| 15 | Medium | High | Medium | Extreme |
| 16 | Medium | Low | Low | Average |
| 17 | Medium | Medium | Low | High |
| 18 | Medium | High | Low | Extreme |
| 19 | Low | Low | High | Average |
| 20 | Low | Medium | High | High |
| 21 | Low | High | High | Extreme |
| 22 | Low | Low | Medium | Average |
| 23 | Low | Medium | Medium | High |
| 24 | Low | High | Medium | Extreme |
| 25 | Low | Low | Low | High |
| 26 | Low | Medium | Low | High |
| 27 | Low | High | Low | Extreme |

(single value) of elevation uncertainty. To acquire a spatially variable estimate of $\delta z$, the above process is applied on a cell-by-cell basis to the entire raster DEM.

To illustrate how this method is conducted for a pairwise DoD calculation, an example from 2006–2005 is shown in Figure 7. Unlike Figure 4, where the probability map was calculated from spatially uniform estimates of $\delta z$ for each DEM, in Figure 7 the $\delta z$ are spatially variable and estimated on a cell-by-cell basis using the FIS. The distinction between the probability maps from a FIS versus a spatially uniform estimate can be difficult to identify visually as the probability values are largely similar overall but with important adjustments of probability values that change their shading. The primary differences are around the fringes of coherent units and these are shown more obviously in thresholded elevation change distributions.

## Spatially coherent erosion and deposition units

A complementary approach to using a FIS to estimate spatial variability in $\delta z$ is based on the observation that erosion and deposition tends to occur in spatially coherent patterns. For example, Figure 2 shows coherent contiguous units of net erosion and net deposition that are generally elongated in a streamwise orientation. Many of the bank erosion units are crescent shaped units with sharp boundaries, whereas many of the depositional units are broader in width and diffuse at their boundaries. If these areas of contiguous and coherent changes could be identified or classified, then DoD predicted elevation changes within those units could be assigned a higher probability of being true, whereas changes in areas without structured patterns of cut and fill could be assigned

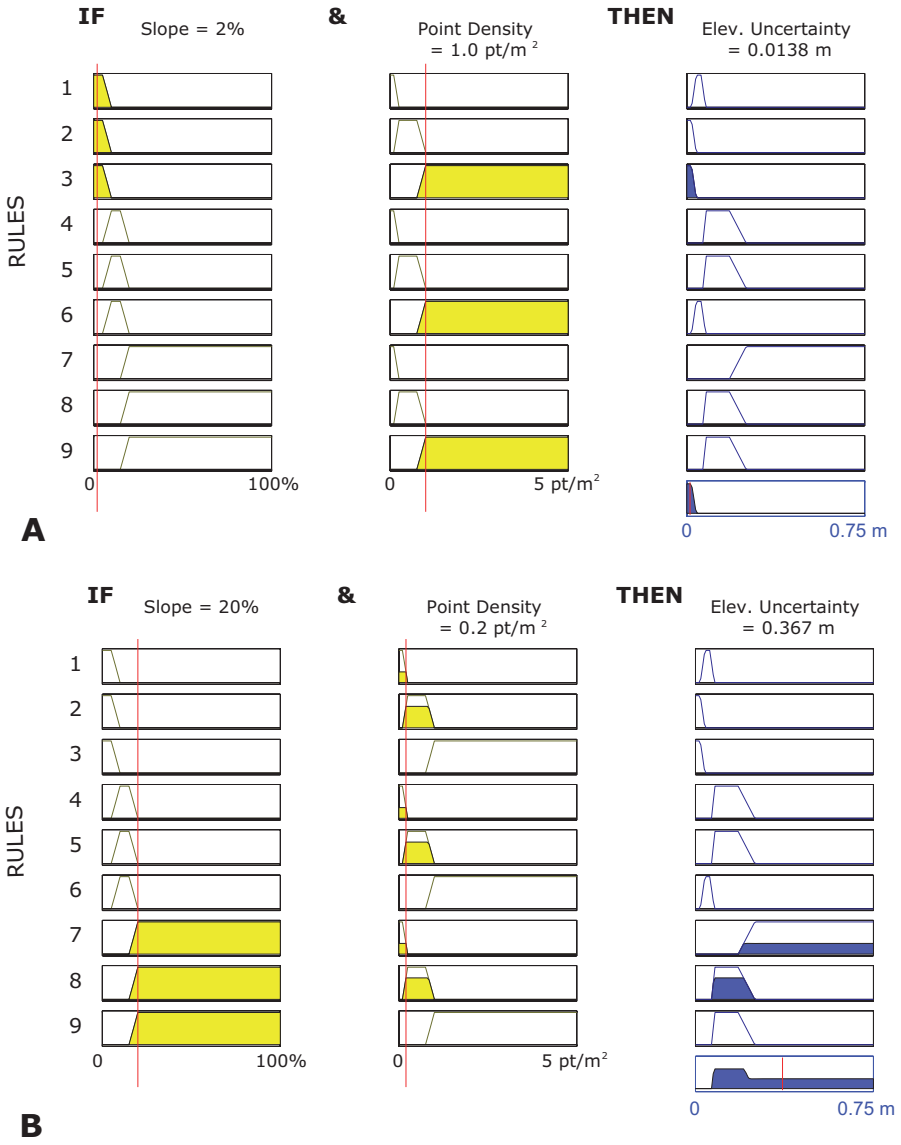


**Figure 6.** Two examples of the total consequence of the two input fuzzy inference system. (A) A 'low' elevation uncertainty situation. (B) A 'high' elevation uncertainty situation. In both situations, the total consequence of the relevant rules are aggregated to the shape that appears in the lower right corner. This aggregated fuzzy output is then defuzzified (using a centroid method) to produce a crisp estimate of elevation uncertainty. The thin red vertical lines represent the input values for the two examples. When a rule is applicable, the mass of the membership function it intersects is highlighted yellow. The output membership function is shaded blue, only when it has two applicable inputs. This figure is available in colour online at www.interscience.wiley.com/journal/espl

to a lower probability. Operationalizing this approach requires: (i) a technique for adjusting the probability estimate accounting for this spatial information; and (ii) a method for segmenting structured patterns of change, from those taken to be random. These methods are described in the next two subsections. If the coherence of such units is ignored, a standard $_{min}$LOD approach leads to a conservative spatial buffer where changes grade from the $_{min}$LOD to zero. Such a buffer is visually evident around units of erosion and deposition and particularly where erosion and deposition units abut each other.

### Defining coherent units

Coherent units are identified using a simple algorithm, which runs a moving window (convolution filter) across the DoD and tallies the number of cells in the window that are erosional or depositional. These counts of erosional and depositional cells are used as indices of spatial contiguity. If a DoD cell is depositional (i.e. positive), and surrounded entirely or primarily by depositional cells (positive), it will have a high spatial contiguity index for deposition and a low contiguity index for erosion. By contrast, if the same depositional DoD cell is surrounded primarily by erosional cells, it will have a low spatial contiguity index for deposition. Separate indices for erosion and deposition are calculated for each cell in the entire grid to avoid the possibility that a particular cell may lie close to a sharp boundary between areas of erosion and deposition (e.g. has the same number of erosion and deposition cells in the window but they are themselves spatially coherent).

After the spatial contiguity indices are calculated for each cell, in any given cell only one of the two indices is used. For cells which the DoD predicts to be erosional, the spatial contiguity index for erosion is used, and vice versa. The index estimates how likely the direction of elevation change is within this spatial neighbourhood (i.e. higher counts more likely, lower counts less likely). A simple linear transform function is used to relate the spatial contiguity index to a probability where $p(A|E_j)$ and $p(A|D_j)$ are the conditional probabilities that cell $j$ is erosional or depositional, respectively, $x$

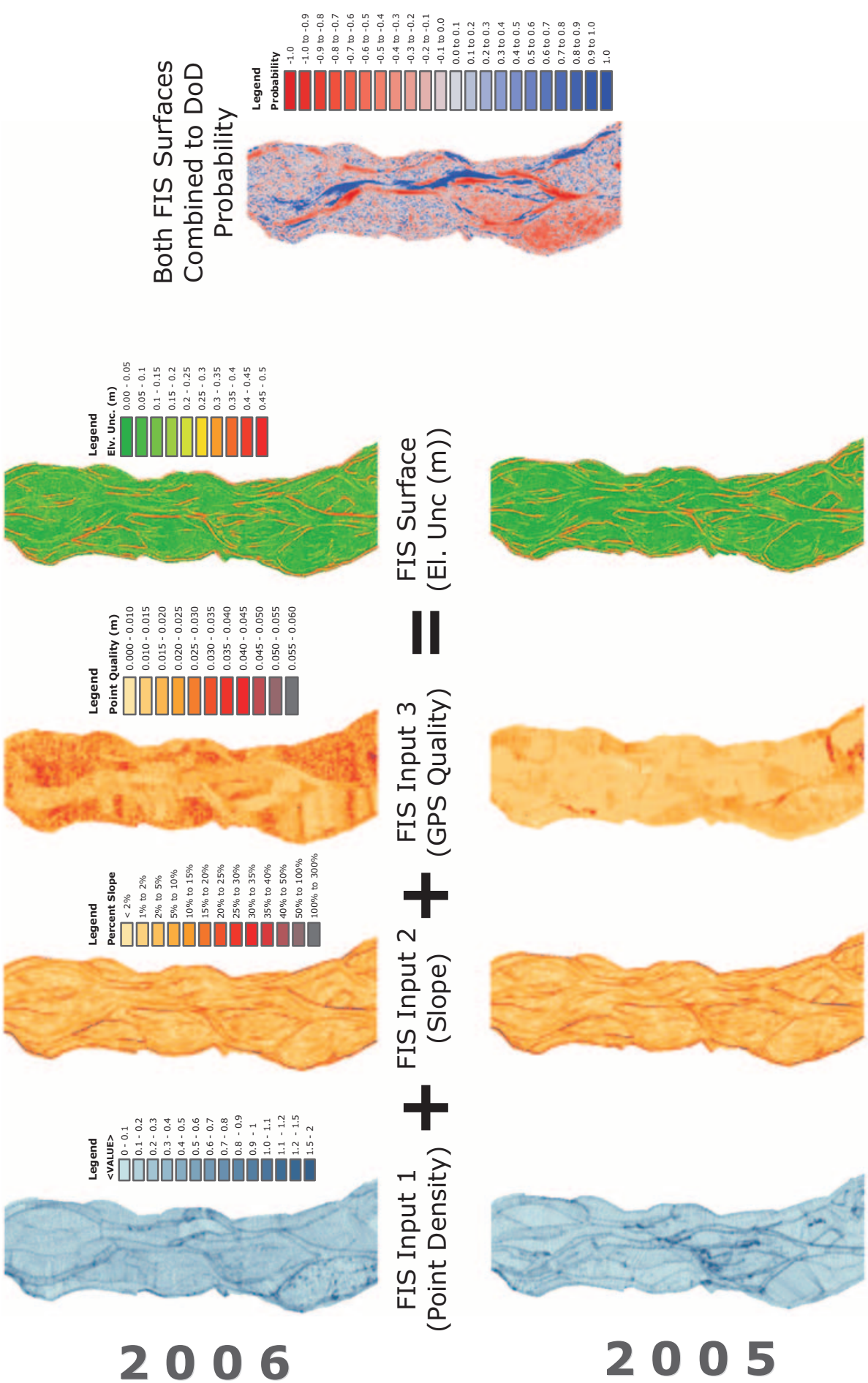


**Figure 7.** Illustration of FIS construction and resulting probability map for 2006–2005 DoD. The top shows the 2006 inputs and the bottom shows the 2005 inputs. The left-hand three inputs combine together as inputs into the three rule FIS to produce the defuzzified FIS prediction of elevation uncertainty. Both predictions of elevation uncertainty combine to produce the probability map that DoD changes are real. Note: El. Unc. is an abbreviation for elevation uncertainty ($\delta z$). This figure is available in colour online at www.interscience.wiley.com/journal/espl

is a unit vector (–1 if cell is erosional, +1 if cell is deposition), and $x_{max}$ and $x_{min}$ are upper and lower thresholds taken to define the number of cells at which the probability becomes 1 and 0 respectively:

$$p(A|E_j) = \frac{\sum_{i=1}^{n=25} x - x_{min}}{x_{max} - x_{min}} \text{ or } p(A|D_j) = \frac{\sum_{i=1}^{n=25} x - x_{min}}{x_{max} - x_{min}} \quad (6)$$

The logic for a transform function can be illustrated with a simple example. If a given cell is calculated to be erosional but its magnitude falls beneath the calculated $_{min}$LoD for that cell, it would normally be discarded. However, if that low-magnitude erosion cell is surrounded by all or primarily erosional cells, then it is highly likely that the cell actually is erosional and the otherwise 'undetectable' change is real. However, if the cell is depositional, and all the cells around it are erosional, it is much less likely the cell is actually depositional. The index of contiguity is linearly transformed into the probability that each cell belongs either to a class of erosion or deposition, as follows (for a 5 × 5 window):

For the analyses reported here, a 5 × 5 cell window was used to define the neighbourhood (reflecting the extent of typical bar-scale features) so that the default value of $x_{max}$ is 25 (i.e. all cells same class). The lower threshold, $x_{min}$ was then taken to be 15. Wheaton (2008) explored the sensitivity of the probability estimate to window size and settled on a default 5 × 5 window size because it was a better discriminator of areas of low magnitude change likely to be real than 3 × 3, 7 × 7 and 9 × 9 windows (Note this result is grid resolution dependent; a 1 m resolution raster was used in this paper).

Updating the probability

Two techniques have been presented for defining a probability that elevation changes are true on the basis of: (a) a spatially uniform estimate of $\delta z$ (e.g. Figure 4) or a spatially variable estimate of $\delta z$ using the FIS (e.g. Figure 7). These estimates could usefully be conjoined with the spatially reliability measure described above, to provide a mixed-method approach to uncertainty estimation. Conjoining these probabilities can be effectively undertaken using Bayes Theorem in which the existing, prior probability is updated using additional information to calculate a conditional probability incorporating both measures. This analysis needs to be conducted for erosion and deposition classes separately, and the results can be combined to produce an overall probability map akin to Figures 4 and 6. Here, the application of Bayes Theorem is described only for the erosional case to illustrate the concepts (it is exactly the same for the depositional case).

The original *a priori* probability ($p(E_j)$) that the DoD predicted elevation change is significant can be updated by calculating a conditional posterior probability ($p(E_j|A)$) that a vertical elevation difference is significant, given the probability ($p(A|E_j)$) revealed from its spatial index analysis. In this case:

$$p(E_j|A) = \frac{p(A|E_j) \cdot p(E_j)}{p(A)} \quad (7)$$

where $p(A)$ is the conditional probability that the cell is erosional given its spatial context within an area of erosion. This is defined as:

$$p(A) = p(A|E_j) \cdot p(E_j) + p(A|E_i) \cdot p(E_i) \quad (8)$$

where the $_j$ subscript refers to a probability that a change is significant and the $_i$ subscript refers to the probability that a change is insignificant Thus, the updated probability can be calculated knowing just two probabilities: the *a priori* probability ($p(E_j)$) and this conditional spatial index probability ($p(A|E_j)$). A simple illustration of this is shown in Figure 8 for the 2006–2005 DoD. When the spatial contiguity index is used with the Bayesian updating, the result is similar to low-pass smoothing of the spatial probability distribution, which highlights coherent regions of change (Burrough and McDonnell, 1998).

## Results

To illustrate the utility of these new methods, they are applied using data from the River Feshie. For comparison, the results of a standard DoD analysis with no uncertainty accounting is presented as a baseline for comparison.

### Unthresholded DoDs

While the DoD maps of Figure 2 are useful for highlighting the spatial pattern and coherence of geomorphic changes, these data can also be quantified in terms of their related elevation change distributions (ECDs) as shown in Figure 9. The areal distributions (left-hand side of Figure 9) are histograms showing the total area experiencing a given magnitude of elevation change in each bin. Without careful inspection, the areal distributions can be somewhat misleading. For the four analysis periods, they all appear to be broadly similar normal distributions roughly centred around an elevation change of zero metres, loosely implying a balance between erosion and deposition (i.e. equilibrium).

By contrast to areal elevation change distributions (ECDs), the volumetric ECDs (right-hand side of Figure 9) are better discriminators of the different styles of change between analysis periods. As the volumetric distribution reflects the area multiplied by the magnitude of elevation change (i.e. the x-axis), the areal and volumetric distributions look quite similar near the middle but are dramatically amplified the further away from zero one gets (i.e. towards higher magnitude changes). As such, the volumetric ECDs are better for resolving signatures of change. The two relatively inactive years (2003 to 2004: Figure 9H and 2005 to 2006: Figure 9D) have relatively similar shape and magnitude, single-peak distributions with a slight degradational bias. The two larger magnitude years (2004 to 2005: Figure 9F and 2006 to 2007: Figure 9B) reveal more complex distributions of change containing at least three peaks. They each have a high peak in the middle centred roughly around zero. 2006 to 2007 is particularly revealing in that it has a very high and concentrated peak of low magnitude deposition with a much more spread-out ridge of erosion spanning a wide range of magnitudes.

These latter characteristics appear to be plausible geomorphic signatures, although the consistently highest magnitude peak centred around zero raises a fundamental question. While it is certainly possible that a high percentage of the areal distribution will be centred about zero, is there necessarily any reason that this phenomena should hold for the volumetric distributions as well? If all the DoD elevation changes in the ECD are assumed to be from geomorphic change (no noise), for the high peak to remain centred around zero in the volumetric distributions would mean that a large relative proportion of the reach would have to be undergoing changes of very low magnitude, because these are being multiplied by such small elevation changes. By contrast, for a peak to

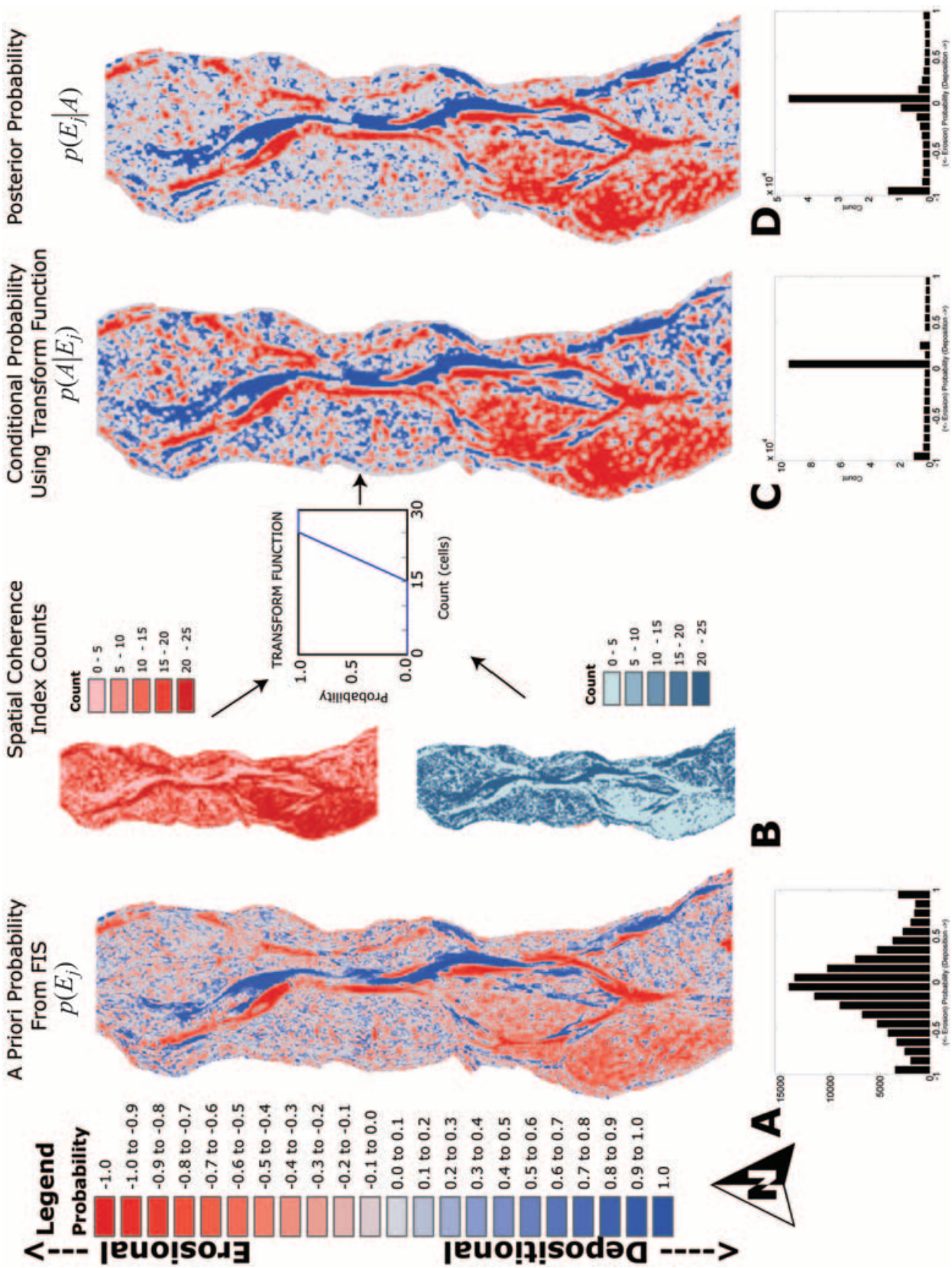


**Figure 8.** Illustration of calculation of Bayesian updating using spatial contiguity index with the 2006–2005 DoD. The a priori probability (in this case estimated using the FIS) is shown in A (spatially on top and probability distribution shown on bottom). Separate spatial indexes are calculated for erosion and deposition (shown in B) and a transform function is used to transfer these to the conditional probability shown in C. Using Bayes thorem, the *a priori* (A) and conditional probability (C) are used to calculate a *posteriori* probability (D). This figure is available in colour online at www.interscience.wiley.com/journal/espl

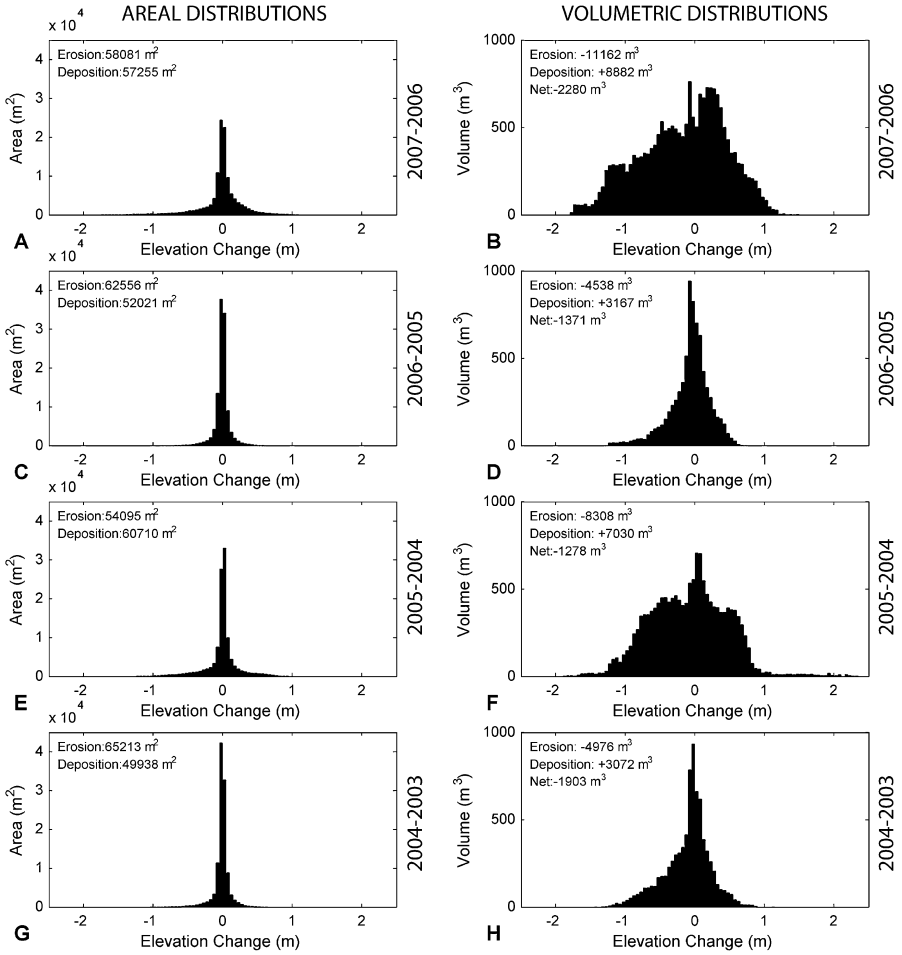


**Figure 9.** Comparison of areal and volumetric DoD Distributions (2007–2003). Each row represents a different analysis period (A and B are 2007–2006; C and D are 2006–2005; E and F are 2005–2004; G and H are 2004–2003). The left-hand column represents the gross unthresholded areal DoD distribution, whereas the right-hand column represents the unthresholded volumetric DoD distribution.

develop around a higher magnitude area, requires a relatively small surface area to change, because these are being multiplied by much larger elevation changes. While there are plausible geomorphic explanations for such a high peak to persist so consistently, this feature is highly suspect in light of the earlier observations regarding the unrealistically high percentage of the reach undergoing changes. Thus, in summary, these DoDs derived from high-quality, high-resolution GPS surveys appear to be producing some reasonable spatial patterns of change (Figure 2), but there are concerns about the reliability of the magnitude and proportions of predicted changes from standard DoD analyses.

## Application of new DoD uncertainty analysis

Figure 10 shows the summary map results of all DoDs thresholded at a 95% confidence interval $_{min}$LoD. The same results are presented in Figure 11 as elevation change distributions. Focusing first on the FIS-only ECDs (Figure 11A), the distribution shapes are different from those simply thresholded using a standard analysis (e.g. Figure 3). Both distributions are bimodal with discrete erosional and depositional distributions. However, in the case of the FIS ECD, the distributions blend more smoothly into the low magnitude changes, instead of just having the central portion excluded. Applying the spatially variable uncertainty analysis has the effect of recovering some information at a lower limit as implied in the membership function of the 'low' $\delta z$ class (Figure 5), but also selectively recovers and discards information across the whole range of elevation change magnitudes. It is conceptually appealing that more conservative thresholds have been applied where $\delta z$ is greater and less conservative thresholds applied where $\delta z$ is less, and the distributions certainly reflect an adjustment based on this principle.

The DoD maps for FIS application (top of Figure 10) measured in comparison with a standard $_{min}$LoD threshold (e.g. Figure 3) show some noticeable improvements in terms of geomorphic plausibility. First, the number of pixelated areas on the floodplain has been reduced dramatically. The primary coherent units of erosion and deposition have dilated around their edges (reflecting lower magnitude changes likely to be true). This has particularly helped improve contiguity between erosion and deposition units, but it could still be improved. Although using the FIS has recovered a small volume of lower magnitude changes, it has not recovered much in the way of meaningful low magnitude elevation changes across the floodplain. This is probably because these changes really are below the lowest $_{min}$LoD limits.

By comparison, applying the spatial coherence index through Bayesian updating (bottom of Figure 10) appears to recover substantial areas of floodplain deposition. Some of the smaller areas appear to be smoothing the highly complex pixelated (assumed random) patterns in the original DoD, however, some of the larger units are in spatially coherent (e.g. splays) and may likely reflect actual overbank deposition. The spatial extent of the individual erosion and deposition units also significantly increases towards the actual extent revealed

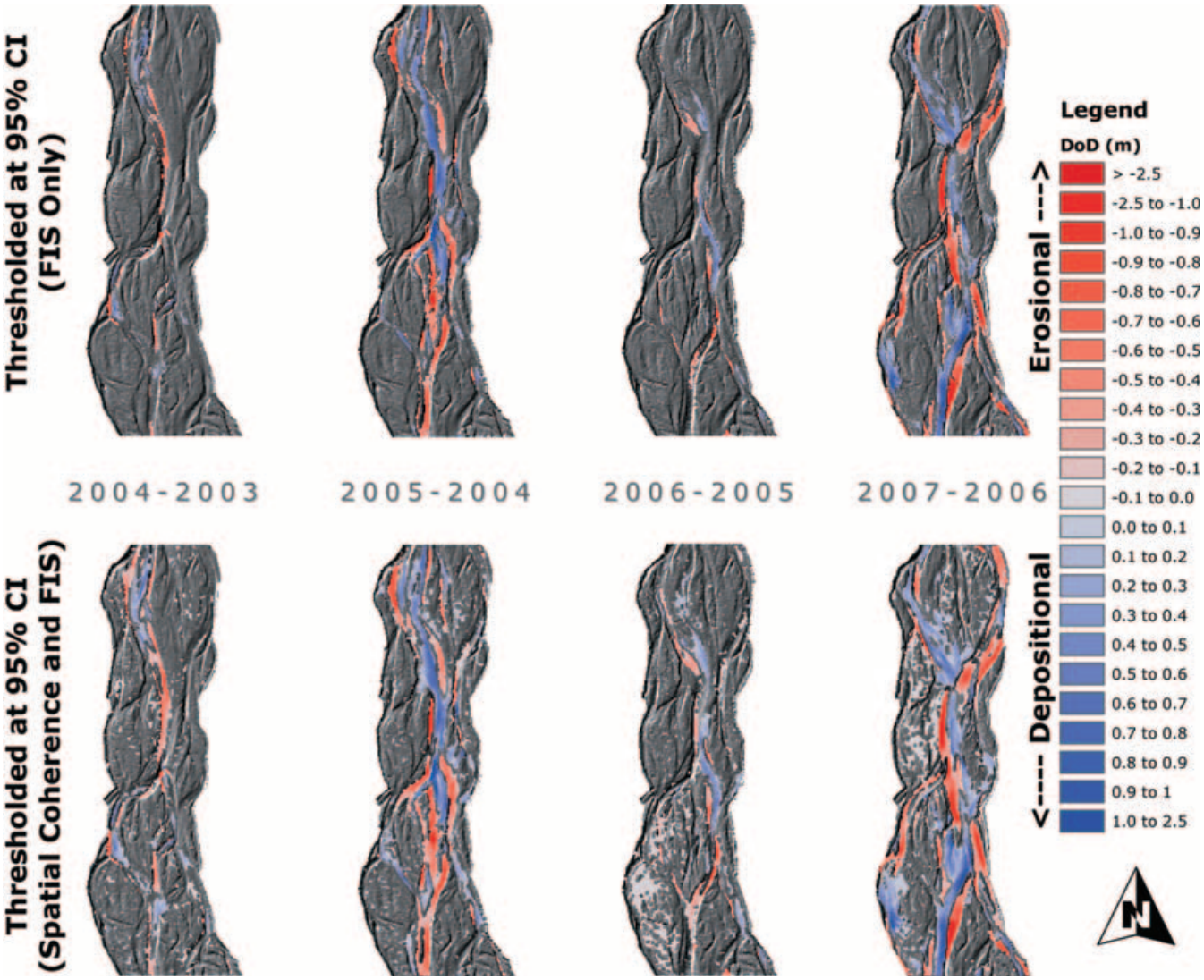


**Figure 10.** Comparison of thresholded DoDs (at 95% Cofidence Interval) based on applying FIS through pathway 3 (top) and applying Bayesian updating using the Spatial Contiguity Index through pathway 4 (bottom) for all annual DoDs from 2007–2003. The hillshade from the more recent year's DEM underlies the DoD for context. This figure is available in colour online at www.interscience.wiley.com/journal/espl

by strong field evidence (facies changes, inundation extents from trashlines, and aerial photos (Wheaton, 2008). Thus, from the DoD maps, the new method qualitatively indicates a substantial improvement.

The ECDs after updating with the spatial coherence index (right-hand side of Figure 11) still emulate the parent distributions from the FIS, as shown on the left-hand side of Figure 11. However, the total volumes have substantially increased over their more simple counterparts, suggesting significant information recovery. This is most pronounced for the two wetter years where greater floodplain inundation was experienced. This is not surprising as this is precisely where a higher degree of low magnitude changes associated with shallow overbank flows are expected to be found. What is particularly promising about the information recovery is not the magnitude of recovery but that it has successfully bridged the gap between the discrete erosional and depositional halves of the distribution, such that even changes close to zero are now represented in the distribution.

To explore to what extent these conclusions hinge on the somewhat arbitrary selection of a reasonably conservative 95% confidence interval, a sensitivity analysis was performed. A total of 44 analyses across the four analysis periods were performed (11 each), in 5% increments from 50% (liberal), up to 95% and then including 99% (conservative). The results are summarized in Figure 12. The original gross budget estimates are plotted in the background as straight lines to give an indication of information loss. The high magnitude years (2007–2006: Figure 12A and 2005–2004: Figure 12C) show much greater sensitivity than the lower magnitude years, particularly above 90%. Once again, 2006–2005 (Figure 12B) shows some sensitivity at higher thresholds to the overall interpretation of net aggradation or degradation. Consistently, the more conservative the confidence interval threshold, the lower volume of change taken to be real. Although the absolute values change, the qualitative interpretation remains consistent above 66%.

Table V summarizes the gross DoD volumes between analyses with: (i) no accounting for uncertainty; (ii) a standard uncertainty analysis; and (iii) the new techniques presented above. The corresponding information loss from the original unthresholded DoD is also reported. Information loss was calculated simply as one minus the ratio of the volume of predicted volumetric change for that uncertainty analysis, divided by the original unthresholded volumetric change. Total information loss refers to the same ratio but is based on the sum of erosion and deposition volumes as opposed to net volumes. Across the information loss statistics for every analysis type, there is only a maximum difference of 8% between

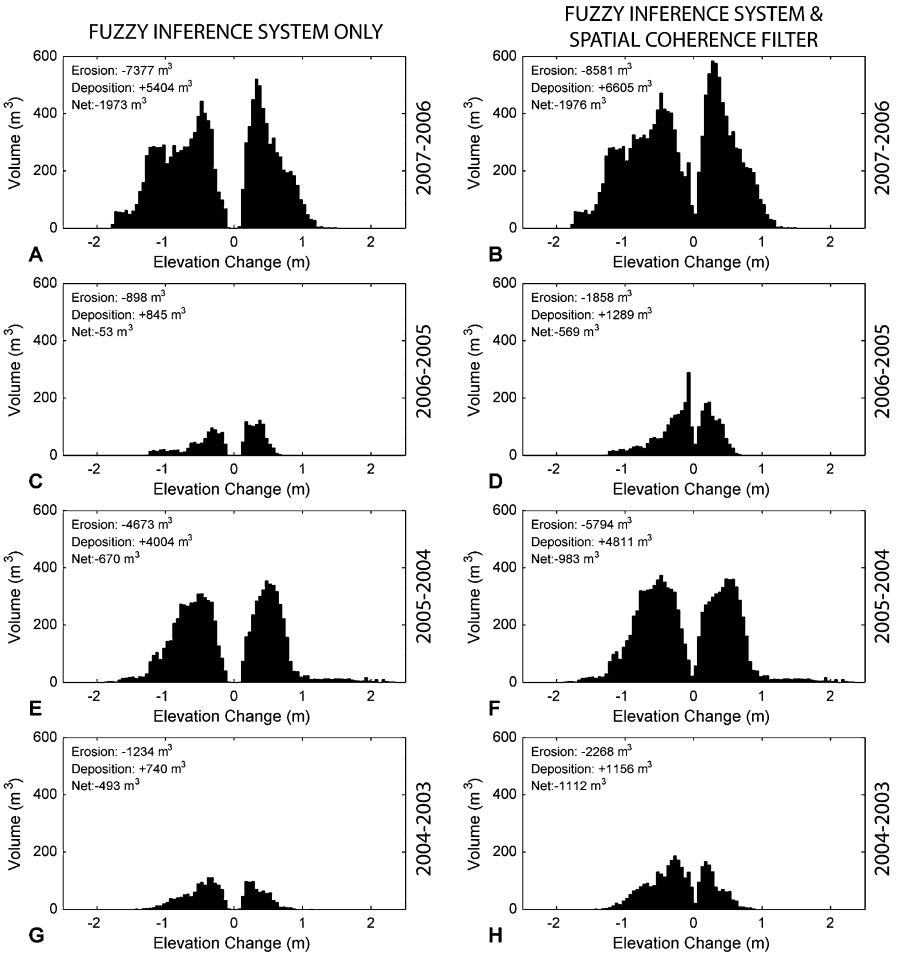


**Figure 11.** Comparison of application of FIS (left) verses FIS with the Spatial Coherence Filter (right) uncertainty algorithms on volumetric DoD elevation change distributions (2007–2003). The left-hand column represents the FIS applied and thresholded at a 95% confidence interval; the right-hand column represents both a FIS and Bayesian updating using the Spatial Contiguity Index applied and thresholded at a 95% confidence interval (see Figure 9).

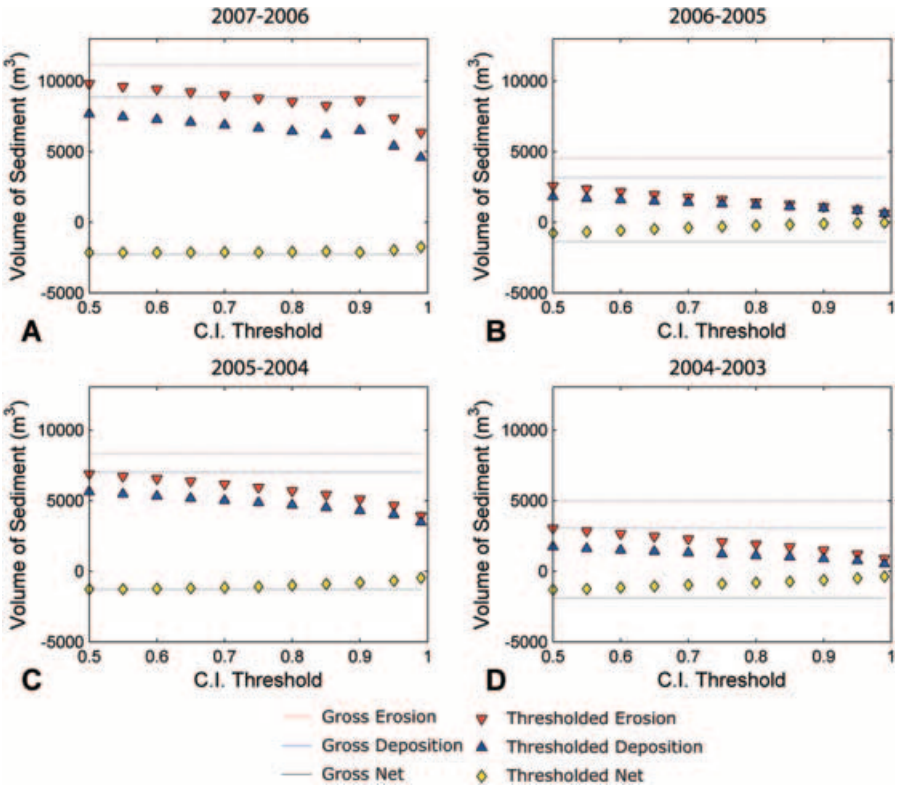


**Figure 12.** An example of pathway 4 sediment budget sensitivity to different confidence interval thresholds. Analysis Intervals: (A) 2007–2006, (B) 2006–2005, (C) 2005–2004, (D) 2004–2003. The gross nonthresholded values are plotted as a series of horizontal reference lines to indicate relative information loss. This figure is available in colour online at www.interscience.wiley.com/journal/espl

**Table V.** Volumetric DoD results and information loss for an unthresholded DoD and three contrasting levels of uncertainty analysis for all years. Mean values across all four periods are also reported. Percentage total loss from original is calculated from the total volume of change, not the net volume of change

| | DoD change | | | Percentage loss from original | | |
|---|---|---|---|---|---|---|
| DoD | Erosion $m^3$ | Deposition $m^3$ | Net $m^3$ | Erosion % | Deposition % | Total % |
| No uncertainty analysis (unthresholded) | | | | | | |
| 2007–2006 | 11162·0 | 8882·3 | –2279·7 | NA | NA | NA |
| 2006–2005 | 4538·5 | 3167·1 | –1371·3 | NA | NA | NA |
| 2005–2004 | 8307·9 | 7029·7 | –1278·2 | NA | NA | NA |
| 2004–2003 | 4975·5 | 3072·2 | –1903·3 | NA | NA | NA |
| μ | 7246·0 | 5537·8 | –1708·2 | NA | NA | NA |
| Standard 10 cm $_{min}$LoD | | | | | | |
| 2007–2006 | 9840·0 | 7687·0 | –2153·0 | 12% | 13% | 13% |
| 2006–2005 | 2771·4 | 1834·8 | –936·6 | 39% | 42% | 40% |
| 2005–2004 | 7220·4 | 5620·7 | –1599·7 | 13% | 20% | 16% |
| 2004–2003 | 3258·8 | 1792·4 | –1466·3 | 35% | 42% | 37% |
| μ | 5772·6 | 4233·7 | –1538·9 | 25% | 29% | 27% |
| FIS only (95% CI) | | | | | | |
| 2007–2006 | 7376·7 | 5403·7 | –1973·0 | 34% | 39% | 36% |
| 2006–2005 | 898·4 | 845·1 | –53·3 | 80% | 73% | 77% |
| 2005–2004 | 4673·4 | 4003·8 | –669·7 | 44% | 43% | 43% |
| 2004–2003 | 1233·5 | 740·5 | –493·1 | 75% | 76% | 75% |
| μ | 3545·5 | 2748·3 | –797·2 | 58% | 58% | 58% |
| Bayesian updating of FIS with spatial coherence (95% CI) | | | | | | |
| 2007–2006 | 8581·0 | 6605·3 | –1975·7 | 23% | 26% | 24% |
| 2006–2005 | 1857·8 | 1288·5 | –569·3 | 59% | 59% | 59% |
| 2005–2004 | 5794·0 | 4810·8 | –983·2 | 30% | 32% | 31% |
| 2004–2003 | 2268·1 | 1156·1 | –1111·9 | 54% | 62% | 57% |
| μ | 4625·2 | 3465·2 | –1160·0 | 42% | 45% | 43% |

erosion, deposition and total information loss, and a mode of 3%. As such, the discussion here will focus only on the total information loss statistic.

Total information loss across all the analyses ranged from as little as 13% to as much as 77% (mean = 40%). Caution should be exercised in interpreting gross information loss as an indication of how well various pathways are performing. These summary results give little insight into what fraction or type of information was 'recovered' or lost like the elevation change distributions do. However, it is difficult to describe overall trends across 24 different elevation change distributions, and for that these statistics can be helpful. Regardless of the uncertainty analysis used, the high magnitude years (2006 to 2007 and 2004 to 2005) consistently produced the lowest information loss (typically roughly half of the other years).

The standard spatially uniform $_{min}$LoD application generally produced the lowest information loss (mean = 27%), but at the expense of geomorphic plausibility and by means of an overly simplistic model of uncertainty. Using the FIS by contrast, generally produced the highest information loss (mean = 58%), but with the aid of a more sophisticated model $\delta z$. When the Bayesian-updated spatial coherence filter is used, much of the information lost from the FIS is recovered (mean = 43%, roughly 16% recovery on average).

# Discussion

## Sensitivity of methods

Although the sensitivity of some of the parameters used in the new methods (e.g. confidence interval, moving window size) have been presented, many other parameters have not been included here (e.g. FIS membership function inputs, DEM grid resolution, ECD bin size, etc.). Appropriate values can be chosen for some of these based on individual circumstances, the nature of the data used (e.g. survey technology, selective/unselective sampling), the type of questions being asked, rules of thumb/previous experience. For example, as a rule of thumb it seems that grain size (e.g. $d_{90}$) could be taken as a rough proxy for the bin interval used in ECDs (default set to 5 cm). Using too high a frequency interval results in rough distributions. Using too coarse an interval makes it difficult to resolve differences that would be the result of a single sheet or layer of grains being deposited (e.g. $2d_{90}$ verses $3d_{90}$). For many intermediate size gravel bed rivers, the default parameter values in the DoD Uncertainty Analysis Software (Matlab scripts) provided with this paper give the user a very reasonable starting point. However, we have included in the software an easy way to perform sensitivity analyses of all parameters as well as to compare six different types of DoD uncertainty analyses including the traditional techniques presented earlier and the new techniques presented here.

## Interpolation errors

In this context, interpolation errors in DEMs manifest themselves primarily in two ways. One is as a result of the TINing process and the other is in the rasterization process. We now consider the questions: are these errors significant and are they dealt with in the DoD uncertainty analyses proposed here?

Recall that TINs are the most common and reliable form of representing high-resolution topographic data, which has

been collected with a topographically stratified sampling scheme to capture morphological grade-breaks (French and Clifford, 2000). The TIN itself is particularly prone to misrepresenting surface topography where low point density and greater topographic complexity combine. The use of an FIS that accounts for both point density and slope is an implicit attempt to account for such TIN interpolations. It is not explicit, in that it does not fundamentally address the root causes of interpolation errors (i.e. over generalization due to lack of points) and does not improve the TIN. All the process does is allow an estimation of the extent to which TIN interpolation errors might be contributing to surface representation uncertainty.

There are further interpolation errors introduced in the process of linearly resampling the TIN onto a raster (grid) DEM. These errors are minimized when a grid resolution is chosen that is similar or finer than the point density of the survey. As point density varies, there is always a trade-off between finer resolution rasters and the associated increased computational overhead. One way to identify appropriate grid resolutions, so as to minimize such interpolation errors, is to look at the sensitivity (through information loss) of DEM budgets to grid resolutions (Brasington *et al.*, 2000). For the Feshie, a 1 m resolution DEM minimized information loss, while maintaining the detail of bar scale morphology and a computationally efficient grid size to perform the numerous analyses reported here. Alternative TIN-based differencing schemes do exist and are used in commercial applications like Surfer and Autodesk's Land Desktop and have been used in the literature (Lane *et al.*, 1994; Lane, 1998; Merz *et al.*, 2006). However, to apply the sort of uncertainty analysis used here, would be algorithmically much more complicated and it would be difficult to maintain flexibility for extension in the future. As such, the simpler raster-based algorithms were adopted here and adequately high grid resolutions were used.

## Application to other survey methods

All of the analyses presented in this paper are based on ground-based survey techniques like rtkGPS and total station surveying. Other popular techniques of monitoring topography include aerial photogrammetry (Westaway *et al.*, 2001; Gilvear *et al.*, 2004), airborne-LiDaR (Charlton *et al.*, 2003; Notebaert *et al.*, 2008) and other optical remote sensing technologies (Marcus and Fonstad, 2008). In addition, terrestrial laser scanning (or ground-based LiDaR) is rapidly emerging as a viable monitoring tool (Brasington *et al.*, 2007; Heritage and Hetherington, 2007; Milan *et al.*, 2007; Heritage and Large, 2009; Hodge *et al.*, 2009a, 2009b), capable of capturing topographic data at resolutions on the order of $10^3$ points $m^{-3}$. All three of these techniques have challenges capturing accurate topography in subaqueous and/or vegetated environments compared with ground-based GPS and total station surveying. However, they can be applied at exceptionally high resolutions over spatial extents similar to that with ground-based methods, or at quite reasonable resolutions over much greater spatial extents (Lane and Chandler, 2003). Increasingly, a mix of surveying technologies is used to build a complete data set for one survey (e.g. mixing GPS and LiDAR data). Also, in a monitoring context, different repeat surveys may have been collected using different techniques. As such, the uncertainty estimation methods here would be much more useful if they could be applied independently to any survey methods, and then propagated into the DoD.

Using a two-rule system, as long as the raw point-data were available from such surveys, the DoD uncertainty techniques developed here should be applicable. Some slight calibration of the membership functions might be needed, but at a minimum these could be calibrated to provide a reasonable (if not conservative) first-order estimate of surface representation uncertainty. However, these estimates could be improved considerably by extending the rule system to factor in data specific to individual survey techniques. For example, most photogrammetry packages provide residuals for each point that could be incorporated, or information from aerial photographs like the presence of vegetation could usefully be incorporated into an FIS rule base. From LiDAR surveys, information about the lag between first and second pulse, could be used not just as a proxy for vegetation height, but explicitly incorporated into the rule system as an uncertainty input. The specific application of the DoD Uncertainty analysis techniques to other survey methods requires further research, but the basic principles should be more generally applicable to detecting any topographic changes captured in repeat topographic surveys. The FIS system alone may also be modified be more generically applicable to estimating surface representation uncertainty for other forms of interpolated spatial data (not just topography).

## Application to non-fluvial environments

The focus here has been on the application of DoD uncertainty techniques to improve morphological sediment budgeting in fluvial environments. There are many other monitoring contexts where DEM-differencing is being used. In civil engineering, comparison of as-built surveys against pre-project surveys has long been used to check cut and fill volumes against grading plans (Webb and Haupt, 2003). In glaciology, repeat topographic surveys are used to perform mass-balance calculations, and to investigate ice calving (Willis *et al.*, 1998; Hubbard *et al.*, 2000; Rippin *et al.*, 2003; Keutterling and Thomas, 2006). In hillslope geomorphology, differencing of LiDAR and photogrammetry surveys can be used to look at geomorphic change from landslides (Eeckhaut *et al.*, 2007; Glenn *et al.*, 2006). Virtually any process that shapes the earth's surface in a manner that produces a magnitude of change larger than minimum detection limits has the potential to be studied using DEM differencing.

As with applying the DoD uncertainty analysis techniques to different surveying technologies, the basic principles should still apply. Specific calibration and/or extension of the rule systems will be necessary, but is straightforward to implement. It is likely that because of the lower resolution of topographic data sources in hillslope geomorphology, glaciology and oceanography applications, more of the budget would be discarded as a result of relatively high minimum levels of detection. All the same, such an analysis is necessary to determine whether anything reliable can be said about change from repeat surveys in such environments. We speculate that this might suggest better quality and higher resolution data sets are necessary for many applications.

## Geomorphic interpretation

In this paper we have focused on the simplistic, gross reach scale interpretations of morphological changes recorded by DoDs that are possible when reliability uncertainty associated with DEM quality are considered robustly. We have only scratched the surface here of a more fundamental structural uncertainty associated with the geomorphic interpretation of

DoD-derived sediment budgets. A wealth of quantitative bar-scale detail about the kinematics of gravel bed rivers are locked up in the high resolution DoDs presented. The spatially variable nature of the DoD uncertainty presented can, however, help to resolve differences in data quality at fine scales, and can be taken further to unlock the wealth of spatially explicit imprints of geomorphic processes in DEMs (Wheaton *et al.*, 2009). Future work should seek to exploit these details to undertake hypothesis testing about mechanisms of change more rigorously.

## Conclusion

This paper has introduced a new technique for quantifying reliability uncertainties from DoDs. The premise for the paper was that there are meaningful low magnitude geomorphic changes being discarded through standard minimum levels of detection analyses that could be better distinguished from noise through a more sophisticated model of DEM surface representation uncertainty. This premise was verified through comparing DoD budgets where a standard spatially uniform analysis was performed, with the more sophisticated analysis, which did indeed recover small magnitude changes in areas where anecdotal field evidence suggested the small changes were coherent and real. The original developments from this paper include the introduction of a spatially variable model of elevation uncertainty based on a flexible and robust fuzzy inference system, and the application of a spatial contiguity index to account for the spatial coherence exhibited in fluvial patterns of erosion and deposition. In addition, simple elevation change distributions were shown to exhibit distinctive signatures of geomorphic change and even in the absence of the more robust uncertainty analysis presented here are a useful and under-utilized tool for assessing DoDs. A series of Matlab scripts, and wizard-dialog user interface are included with this paper so readers can apply the methods themselves.

The new approach was applied to 5 years of high resolution repeat annual GPS surveys of a partially-braided portion of the River Feshie, in the Cairngorm Mountains of Scotland. The DoD uncertainty analysis tools are simple to apply to any topographic data set and the underlying rule systems are straightforward to calibrate to different field settings. The analysis framework is designed to give a robust spatially-variable estimate of DEM uncertainty from any raw topographic point data. However, the framework is flexible and easy to extend to include more rules and factors (e.g. roughness) known to influence surface representation uncertainty if they are available.

*Acknowledgements*—The authors are grateful to the numerous individuals who assisted in the data collection on the Feshie over the past 8 years from Aberystwyth University, University of Southampton, University of Cambridge, and Glasgow University. In particular, Clare Cox, Dr Rebecca Hodges, and Richard Williams were instrumental in the surveying work. This research was primarily funded by a PhD studentship for the lead author at the University of Southampton, paid for jointly by the School of Geography and Centre for Ecology and Hydrology, with international fees covered by an Overseas Research Studentship from Universities UK. The field work was also supported by a Horton Hydrology Research Grant from the American Geophysical Union, and an Aberystwyth University Research Fund Award. Further staff time, travel and equipment were generously provided by Centre for Catchment and Coastal Research, the Institute of Geography and Earth Sciences at Aberystwyth University as well as the Department of Geography at University of Cambridge.

## References

Bandemer H, Gottwald S. 1995. *Fuzzy Sets, Fuzzy Logic, Fuzzy Methods: with Applications*. John Wiley and Sons: Chichester.

Brasington J, Rumsby BT, Mcvey RA. 2000. Monitoring and modelling morphological change in a braided gravel-bed river using high resolution GPS-based survey. *Earth Surface Processes and Landforms* **25**(9): 973–990. DOI: 10.1002/1096-9837(200008)25:9<973::AIDESP111>3.0.CO;2-Y

Brasington J, Langham J, Rumsby B. 2003. Methodological sensitivity of morphometric estimates of coarse fluvial sediment transport. *Geomorphology* **53**(3–4): 299–316. DOI: 10.1016/S0169-555X(02)00320-3

Brasington J, Wheaton JM, Vericat D, Hodge R. 2007. Modelling braided river morphodynamics with terrestrial laser scanning. *EOS Transactions AGU* **88**(52): Fall Meet. Suppl., Abstract H51L-02.

Brazier V, Ballantyne CK. 1989. Late Holocene debris cone evolution in Glen Feshie, western Cairngorm Mountains, Scotland. *Transactions of the Royal Society of Edinburgh: Earth Sciences* **80**: 17–24.

Bremner A. 1915. The capture of the Geldie by the Feshie. *Scottish Geographical Magazine* **31**: 589–596.

Brewer PA, Passmore DG. 2002. Sediment budgeting techniques in gravel bed rivers. In *Sediment Flux to Basins: Causes, Controls and Consequences, Special Publication 191*, Jones S, Frostick L (eds). Geological Society: London; 97–113.

Burrough PA, McDonnell RA. 1998. *Principles of Geographical Information Systems: Spatial Information Systems and Geostatistics*. Oxford University Press: Oxford.

Calder BR, Mayer LA. 2003. Automatic processing of high-rate, high-density multibeam echosounder data. *Geochemistry, Geophysics, Geosystems* **4**(6): 1048. DOI: 10.1029/2002GC000486.

Carter WE, Shrestha RL, Slatton KC. 2007. Geodetic laser scanning. *Physics Today* **60**(12): 41–47.

Cavalli M, Tarolli P, Marchi L, Dalla Fontana G. 2008. The effectiveness of airborne LiDAR data in the recognition of channel-bed morphology. *CATENA* **73**(3): 249–260. DOI: 10.1016/j.catena.2007.11.001.

Chappell A, Heritage GL, Fuller IC, Large ARG, Milan DJ. 2003. Geostatistical analysis of ground-survey elevation data to elucidate spatial and temporal river channel change. *Earth Surface Processes and Landforms* **28**(4): 349–370. DOI: 10.1002/esp.444.

Charlton ME, Large ARG, Fuller IC. 2003. Application of airborne LiDAR in river environments: The River Coquet, Northumberland, UK. *Earth Surface Processes and Landforms* **28**(3): 299–306. DOI: 10.1002/esp.482.

Chen S, Nikolaidis E, Cudney HH, Rosca R, Haftka RT. 1999. *Comparison of Probabilistic and Fuzzy Set Methods for Designing under Uncertainty*. AIAA-99-1579, American Institute of Aeronautics and Astronautics.

Church M, Ashmore P. 1998. Sediment transport and river morphology: a paradigm for study. In *Gravel-Bed Rivers in the Environment*, Klingeman PC (ed). Water Resources Center: Highlands Ranch, CO.

Eeckhaut MVD, Poesen J, Verstraeten G, Vanacker V, Moeyersons J, Nyssen J, Beek LPHv, Vandekerckhove L. 2007. Use of LIDAR-derived images for mapping old landslides under forest. *Earth Surface Processes and Landforms* **32**(5): 754–769. DOI: 10.1002/esp.1417.

Ferguson RI, Werritty A. 1983. Bar development and channel changes in the gravelly River Feshie, Scotland. *International Association of Sedimentologists Special Publications* **6**: 181–193.

Ferguson RI, Ashworth PJ. 1992. Spatial patterns of bedload transport and channel change in braided and near-braided rivers. In *Dynamics of Gravel-bed Rivers*, Billi P, Hey RD, Thorne CR, Tacconi P (eds). Wiley: Chichester; 477–496.

French JR, Clifford NJ. 2000. Hydrodynamic modeling as a basis for explaining estuarine environmental dynamics: some computational and methodological issues. *Hydrological Processes* **14**: 2089–2108. DOI: 10.1002/1099-1085(20000815/30)14:11/12<2089::AIDHYP56>3.0.CO;2-L.

Fuller IC, Large ARG, Charlton ME, Heritage GL, Milan DJ. 2003. Reach-scale sediment transfers: An evaluation of two morphological budgeting approaches. *Earth Surface Processes and Landforms* **28**(8): 889–903. DOI: 10.1002/esp.1011.

Gilvear DJ, Cecil J, Parsons H. 2000. Channel change and vegetation diversity on a low-angle alluvial fan, River Feshie, Scotland. *Aquatic Conservation-Marine and Freshwater Ecosystems* **10**(1): 53–71.

Gilvear DJ, Davids C, Tyler AN. 2004. The use of remotely sensed data to detect channel hydromorphology; River Tummel, Scotland. *River Research and Applications* **20**(7): 795–811. DOI: 10.1002/rra.792.

Glenn NF, Streutker DR, Chadwick DJ, Thackray GD, Dorsch SJ. 2006. Analysis of LiDARderived topographic information for characterizing and differentiating landslide morphology and activity. *Geomorphology* **73**(1–2): 131–148. DOI: 10.1016/j.geomorph.2005.07.006

Heritage G, Hetherington D. 2007. Towards a protocol for laser scanning in fluvial geomorphology. *Earth Surface Processes and Landforms* **32**(1): 66–74. DOI: 10.1002/esp.1375.

Heritage G, Large ARG (eds). 2009. *Laser Scanning for the Environmental Sciences*. Wiley: Chichester.

Hodge R, Brasington J, Richards K. 2009a. Analysing laser-scanned digital terrain models of gravel bed surfaces: linking morphology to sediment transport processes and hydraulics. *Sedimentology*. DOI: 10.1111/j.1365-3091.2009.01068.x.

Hodge RA, Brasington J, Richards KS. 2009b. In-situ characterisation of grain-scale fluvial morphology using Terrestrial Laser Scanning. *Earth Surface Processes and Landforms* **34**(7): 954–968. DOI: 10.1002/esp.1780.

Hubbard A, Willis I, Sharp M, Mair D, Nienow P, Hubbard B, Blatter H. 2000. Glacier massbalance determination by remote sensing and high-resolution modelling. *Journal of Glaciology* **46**(154): 491–498. DOI: 10.3189/172756500781833016.

Jang JSR, Gulley N. 2007. *Fuzzy Logic Toolbox 2: User Guide, Matlab*, Matlab, Natick, MA, 299 pp. Available at: http://www.mathworks.com/access/helpdesk/help/pdf_doc/fuzzy/fuzzy.pdf.

Jang JSR, Gulley N. 2009. *Fuzzy Logic Toolbox 2: User Guide, Matlab*, Matlab, Natick, MA, 343 pp. Available at: http://www.mathworks.com/access/helpdesk/help/pdf_doc/fuzzy/fuzzy.pdf.

Keutterling A, Thomas A. 2006. Monitoring glacier elevation and volume changes with digital photogrammetry and GIS at Gepatschferner glacier, Austria. *International Journal of Remote Sensing* **27**(19): 4371–4380. DOI: 10.1080/01431160600851819.

Klir GJ, Yuan B. 1995. *Fuzzy Sets and Fuzzy Logic: Theory and Applications*. Prentice Hall: Upper Saddle River, NJ.

Lane SN. 1998. The use of digital terrain modelling in the understanding of dynamic river channel systems. In *Landform Monitoring, Modelling and Analysis*, Lane SN, Richards K, Chandler J (eds). Wiley: Chichester; 311–342.

Lane SN, Chandler JH. 2003. Editorial: The generation of high quality topographic data for hydrology and geomorphology: new data sources, new applications and new problems. *Earth Surface Processes and Landforms* **28**(3): 229–230. DOI: 10.1002/esp.479.

Lane SN, Chandler JH, Richards KS. 1994. Developments in monitoring and modeling small-scale river bed topography. *Earth Surface Processes and Landforms* **19**(4): 349–368. DOI: 10.1002/esp.3290190406.

Lane SN, Westaway RM, Hicks DM. 2003. Estimation of erosion and deposition volumes in a large, gravel-bed, braided river using synoptic remote sensing. *Earth Surface Processes and Landforms* **28**(3): 249–271. DOI: 10.1002/esp.483.

Lichti DD, Gordon SJ, Tipdecho T. 2005. Error models and propagation in directly georeferenced terrestrial laser scanner networks. *Journal of Surveying Engineering-ASCE* **131**(4): 135–142. DOI: 10.1061/(ASCE)0733-9453(2005)131:4(135).

Lodwick WA, Santos J. 2003. Constructing consistent fuzzy surfaces from fuzzy data. *Fuzzy Sets and Systems* **135**: 259–277. DOI: 10.1016/S0165-0114(02)00139-2.

Marcus WA, Fonstad MA. 2008. Optical remote mapping of rivers at sub-meter resolutions and watershed extents. *Earth Surface Processes and Landforms* **33**(1): 4–24.

McKean JA, Isaak DJ, Wright CW. 2008. Geomorphic controls on salmon nesting patterns described by a new, narrow-beam terrestrial–aquatic lidar. *Ecological Society of America* **6**(3): 125–130. DOI: 10.1890/070109.

Merz JE, Pasternack GB, Wheaton JM. 2006. Sediment budget for salmonid spawning habitat rehabilitation in a regulated river. *Geomorphology* **76**(1–2): 207–228. DOI: 10.1016/j.geomorph.2005.11.004.

Milan DJ, Heritage GL, Hetherington D. 2007. Application of a 3D laser scanner in the assessment of erosion and deposition volumes and channel change in a proglacial river. *Earth Surface Processes and Landforms* **32**(11): 1657–1674. DOI: 10.1002/esp.1592.

Milne JA, Sear D. 1997. Modelling river channel topography using GIS. *International Journal of Geographical Information Science* **11**(5): 499–519. DOI: 10.1080/136588197242275.

Notebaert B, Verstraeten G, Govers G, Poesen J. 2008. Qualitative and quantitative applications of LiDAR imagery in fluvial geomorphology. *Earth Surface Processes and Landforms* **34**(2): 217–231. DOI: 10.1002/esp.1705.

Rippin D, Willis I, Arnold N, Hodson A, Moore J, Kohler J, Bjornsson H. 2003. Changes in geometry and subglacial drainage of Midre Lovenbreen, Svalbard, determined from digital elevation models. *Earth Surface Processes and Landforms* **28**(3): 273–298. DOI: 10.1002/esp.485.

Robertson-Rintoul MSE. 1986. A quantitative soil-stratigraphic approach to the correlation and dating of post-glacial river terraces in Glen Feshie, western Cairngorms. *Earth Surface Processes and Landforms* **11**(6): 605–617.

Rodgers P, Soulsby C, Petry J, Malcolm I, Gibbins C, Dunn S. 2004. Groundwater-surface-water interactions in a braided river: a tracer-based assessment. *Hydrological Processes* **18**(7): 1315–1332.

Rodgers P, Soulsby C, Waldron S. 2005. Stable isotope tracers as diagnostic tools in upscaling flow path understanding and residence time estimates in a mountainous mesoscale catchment. *Hydrological Processes* **19**(11): 2291–2307.

Rumsby B, McVey R, Brasington J. 2001. 16. The Potential for high resolution fluvial archives in braided rivers: quantifying historic reach-scale channel and floodplain development in the River Feshie, Scotland. In *River Basin Sediment Systems: Archives of Environmental Change*, Maddy D, Macklin MG, Woodard JC (eds). A.A. Balkema Publishers: Steenwijk, The Netherlands; 445–467.

Rumsby BT, Brasington J, Langham JA, McLelland SJ, Middleton R, Rollinson G. 2008. Monitoring and modelling particle and reach-scale morphological change in gravel-bed rivers: Applications and challenges. *Geomorphology* **93**(1–2): 40–54. DOI: 10.1016/j.geomorph.2006.12.017.

Sear DA, Milne JA. 2000. Surface modelling of upland river channel topography and sedimentology using GIS. *Physics and Chemistry of the Earth Part B-Hydrology Oceans and Atmosphere* **25**(4): 399–406. DOI: 10.1016/S1464-1909(00)00033-2.

Soulsby C, Malcolm R, Gibbins C, Dilks C. 2001. Seasonality, water quality trends and biological responses in four streams in the Cairngorm Mountains, Scotland. *Hydrology and Earth System Sciences* **5**(3): 433–450.

Soulsby C, Tetzlaff D, Rodgers P, Dunn S, Waldron S. 2006. Runoff processes, stream water residence times and controlling landscape characteristics in a mesoscale catchment: an initial evaluation. *Journal of Hydrology* **325**(1–4): 197–221.

Taylor J. 1997. *An Introduction to Error Analysis: the Study of Uncertainties in Physical Measurements*, 2nd edn. University Science Books: Sausalito, CA.

Thomas RE. 2006. *Flow Processes and Channel Change in Sand-Bedded Braided Rivers*. PhD thesis, University of Leeds, Leeds, UK. Available at: http://homepages.see.leeds.ac.uk/~georet/projects/Thesis.pdf.

Valle BL, Pasternack GB. 2005. Field mapping and digital elevation models of two hydraulic jump regions in a step-pool mountain channel. *Earth Surface Processes and Landforms* **31**(6): 646–664.

Webb RM, Haupt TC. 2003. The potential of 4D CAD as a tool for construction management. In *4D CAD and Visualization in Construction: Developments and Applications*, Issa RRA, Flood I, O'Brien WJ (eds). Taylor & Francis; 227–243.

Wechsler SP. 2003. Perceptions of digital elevation model uncertainty by DEM users. *URISA Journal* **15**(2): 57–64.

Wechsler SP, Kroll CN. 2006. Quantifying DEM uncertainty and its effect on topographic parameters. *Photogrammetric Engineering and Remote Sensing* **72**(9): 1081–1090.

Werrity A, Ferguson RI. 1980. Pattern change in a Scottish braided river over 1, 30 and 200 years. In *Timescales in Geomorphology*,

 

Cullingford RA, Davidson DA, Lewin J (eds). Wiley: Chichester; 53–68.

Westaway RM, Lane SN, Hicks DM. 2001. Remote sensing of clear-water, shallow, gravel-bed rivers using digital photogrammetry. *Photogrammetric Engineering and Remote Sensing* **67**(11): 1271–1281.

Westaway RM, Lane SN, Hicks DM. 2003. Remote survey of large-scale braided, gravel-bed rivers using digital photogrammetry and image analysis. *International Journal of Remote Sensing* **24**(4): 795–815. DOI: 10.1080/01431160110113070.

Wheaton JM. 2008. Uncertainty in morphological sediment budgeting of rivers. Unpublished PhD, University of Southampton, Southampton, 412 pp. Available at: http://www.joewheaton.org/Home/research/projects-1/phdthesis

Wheaton JM, Brasington J, Darby SE, Merz JE, Pasterneck GB, Sear DA, Vericat D. 2009. Linking geomorphic changes to salmonid habitat at a scale relevant to fish. *River Research and Applications* DOI: 10.1002/rra.1305.

Wheaton JM, Brasington J, Williams RD. 2004. Modelling fluvial sediment budgets under uncertainty. *EOS Transactions AGU* **85**(47): Fall Meeting Supplement, Abstract H53C-1264.

Willis IC, Arnold NS, Sharp MJ, Bonvin J-M, Hubbard B. 1998. Mass balance and flow variations of Haut Glacier d'Arolla, Switzerland, calculated using digital terrain modelling techniques. In *Landform Monitoring, Modelling and Analysis*, Lane SN, Richards K, Chandler J (eds). Wiley: Chichester; 343–361.

Winterbottom SJ, Gilvear DJ. 1997. Quantification of channel bed morphology in gravel-bed rivers using airborne multispectral imagery and aerial photography. *Regulated Rivers-Research & Management* **13**(6): 489–499.

Wise SM. 1998. The effect of GIS interpolation errors on the use of digital elevation models in geomorphology. In *Landform Monitoring, Modelling and Analysis*, Lane SN, Richards K, Chandler J (eds). Wiley: Chichester; 139–164.

Young JAT. 1976. The terraces of Glen Feshie, Inverness-shire. *Transactions of the Royal Society of Edinburgh: Earth Sciences* **69**: 501–512.